12

J-ADAPTIVE ESTIMATION WITH ESTIMATED NOISE STATISTICS

Andrew H. Jazwinski and Conrad Hipkins
Business and Technological Systems, Inc.
10210 Greenbelt Road, Suite 605
Seabrook, Maryland 20801

November 1973

Final Report BTS-TR-73-5

Prepared for

GODDARD SPACE FLIGHT CENTER
Greenbelt, Maryland 20771

1. Report No.	2. Government Accession No.	3. Recipient's Catalog No.

4. Title and Subtitle	5. Report Date
J-ADAPTIVE ESTIMATION WITH ESTIMATED NOISE STATISTICS	November 1973
	6. Performing Organization Code
7. Author(s)	8. Performing Organization Report No.
Andrew H. Jazwinski and Conrad Hipkins	BTS-TR-73-5
9. Performing Organization Name and Address	10. Work Unit No.
Business and Technological Systems, Inc. 10210 Greenbelt Road, Suite 605 Seabrook, Maryland 20801	11. Contract or Grant No. NAS 5-22144
	13. Type of Report and Period Covered
12. Sponsoring Agency Name and Address	Final Report
GODDARD SPACE FLIGHT CENTER Greenbelt, Maryland 20771 Mr. Eugene J. Lefferts	14. Sponsoring Agency Code

15. Supplementary Notes

16. Abstract

The previously developed J-Adaptive sequential estimator is extended to include simultaneous estimation of the noise statistics in a statistical model for unmodeled system dynamics. This extension completely automates the estimator, eliminating the requirement of an analyst in the loop. Simulations in satellite orbit determination demonstrate the efficacy of the sequential estimation algorithm.

17. Key Words (Selected by Author(s))	18. Distribution Statement
Estimation, Filtering, Adaptive Filtering, Orbit Determination Identification	

19. Security Classif. (of this report)	20. Security Classif. (of this page)	21. No. of Pages	22. Price*
Unclassified	Unclassified	~~44~~ 43	4.50

*For sale by the Clearinghouse for Federal Scientific and Technical Information, Springfield, Virginia 22151.

TABLE OF CONTENTS

		Page
I.	INTRODUCTION	1
II.	THE J-ADAPTIVE ESTIMATOR	3
III.	ESTIMATION OF NOISE STATISTICS	5
IV.	DETAILS OF SIMULATIONS	11
V.	SIMULATION RESULTS	13
VI.	NEW TECHNOLOGY	37
VII.	CONCLUSIONS AND RECOMMENDATIONS	39
VIII.	REFERENCES	41
	Appendix A - Oblateness Model	43

LIST OF FIGURES

Figure 1. TRACKING THE x-ACCELERATION
($\hat{q}$; 2-body model; σ_ρ = 3m, $\sigma_{\dot{\rho}}$ = 1 cm/sec)

Figure 2. TRACKING THE y-ACCELERATION
($\hat{q}$; 2-body model; σ_ρ = 3m, $\sigma_{\dot{\rho}}$ = 1 cm/sec)

Figure 3. TRACKING THE z-ACCELERATION
($\hat{q}$; 2-body model; σ_ρ = 3m, $\sigma_{\dot{\rho}}$ = 1 cm/sec)

Figure 4. NORMALIZED RANGE RESIDUALS
($\hat{q}$; 2-body model; σ_ρ = 3m, $\sigma_{\dot{\rho}}$ = 1 cm/sec)

Figure 5. NORMALIZED RANGE RATE RESIDUALS
($\hat{q}$; 2-body model; σ_ρ = 3m, $\sigma_{\dot{\rho}}$ = 1 cm/sec)

Figure 6. POSITION ESTIMATION ERRORS
($\hat{q}$; 2-body model; σ_ρ = 3m, $\sigma_{\dot{\rho}}$ = 1 cm/sec)

Figure 7. VELOCITY ESTIMATION ERRORS
($\hat{q}$; 2-body model; σ_ρ = 3m, $\sigma_{\dot{\rho}}$ = 1 cm/sec)

Figure 8. TRACKING THE x-ACCELERATION
($\hat{q}$; 2-body model; σ_ρ = 0.3m, $\sigma_{\dot{\rho}}$ = 0.1 cm/sec)

Figure 9. TRACKING THE x-ACCELERATION
($\bar{U}$; 2-body model; σ_ρ = 3m, $\sigma_{\dot{\rho}}$ = 1 cm/sec)

Figure 10. NORMALIZED RANGE RATE RESIDUALS
($\bar{U}$; 2-body model; σ_ρ = 3m, $\sigma_{\dot{\rho}}$ = 1 cm/sec)

Figure 11. TRACKING THE z-ACCELERATION - LOG SCALE
($\hat{q}$; J_2, J_3 model; σ_ρ = 3m, $\sigma_{\dot{\rho}}$ = 1 cm/sec)

Figure 12. POSITION ESTIMATION ERRORS
($\hat{q}$; J_2, J_3 model; σ_ρ = 3m, $\sigma_{\dot{\rho}}$ = 1 cm/sec)

Figure 13. VELOCITY ESTIMATION ERRORS
($\hat{q}$; J_2, J_3 model; σ_ρ = 3m, $\sigma_{\dot{\rho}}$ = 1 cm/sec)

Figure 14. TRACKING THE z-ACCELERATION - LOG SCALE
($\hat{q}$; J_2, J_3 model; σ_ρ = 0.3m, $\sigma_{\dot{\rho}}$ = 0.1 cm/sec)

Figure 15. TRACKING THE z-ACCELERATION
($\hat{q}$; J_2, J_3 model; σ_ρ = 0.3m, $\sigma_{\dot{\rho}}$ = 0.1 cm/sec)

Figure 16. TRACKING THE z-ACCELERATION - LOG SCALE
($\hat{q}$; J_2, J_3 model; σ_ρ = 3cm, $\sigma_{\dot{\rho}}$ = 0.01 cm/sec)

Figure 17. MASCON x-ACCELERATION
($\hat{q}$; Unmodeled mascon; σ_ρ = 1 cm, $\sigma_{\dot{\rho}}$ = 0.01 cm/sec)

Figure 18. MASCON x-ACCELERATION
($\bar{U}$; Unmodeled mascon; σ_ρ = 1cm, $\sigma_{\dot{\rho}}$ = 0.01 cm/sec)

I. INTRODUCTION

In previous works[1,2] the authors have described a sequential estimator (called the J-Adaptive estimator) which tracks the state of a dynamical system with a simplified system model by simultaneously tracking a forcing term which approximates the unmodeled system dynamics. This estimator has been very successfully simulated in satellite orbit determination problems[1], where the unmodeled system dynamics result from unmodeled earth oblateness accelerations. The J-Adaptive estimator requires, however, the specification of a statistical model for the unmodeled system dynamics.

The present study extends the J-Adaptive Estimator to include the simultaneous estimation of the statistics of the unmodeled system accelerations, thus completely automating the estimation process. Simulations in satellite orbit determination demonstrate the effectiveness of the resulting estimator.

The report is organized as follows. Section II reviews the J-Adaptive estimation concepts previously reported in detail. The algorithm for estimating the unmodeled acceleration noise statistics is presented in Section III, which also gives the full estimator equations. Section IV presents the simulation results in detail. Finally, Section VII presents the conclusions of this study and recommendations for further work.

II. THE J-ADAPTIVE ESTIMATOR

The basic concepts behind the J-Adaptive estimator have been reported previously.[1,2] In essence, the real dynamical system

$$\ddot{R} = f(R,\dot{R}), \tag{1}$$

where R is the satellite position vector ($\dot{R} = V$), is modeled in the estimator as

$$\ddot{R} = f_m(R,\dot{R}) + S(t)u, \tag{2}$$

so that $S(t)u$ approximates

$$f(R,\dot{R}) - f_m(R,\dot{R}), \tag{3}$$

which is the modeling error made in the estimator dynamics. $S(t)$ is a specified "symmetry" matrix (not contained in the work reported in Ref [1]), and u is the unmodeled acceleration vector.

The J-Adaptive estimator sequentially tracks the state R,V and the unmodeled acceleration vector u from tracking (or other) data. In the estimator, the unmodeled acceleration u is modeled statistically as a random polynomial in time (see Ref [1] and Section III). The equations for the basic J-Adaptive estimator are given in Eqs (24-29) of Ref [1]. The inclusion of the symmetry matrix S modifies the prediction equation for the state estimate $\hat{x}$ (first of Eqs (24) of Ref [1]), and the definitions of the ψ, ψ_d and ψ_{dd} matrices of Eqs (14) of Ref [1], which now become

$$\psi(i+1,i) = \begin{bmatrix} \frac{\tau^2}{2} S \\ \tau S \end{bmatrix}, \quad \psi_d(i+1,i) = \begin{bmatrix} \frac{\tau^3}{6} S \\ \frac{\tau^2}{2} S \end{bmatrix}, \quad \psi_{dd}(i+1,i) = \begin{bmatrix} \frac{\tau^4}{24} S \\ \frac{\tau^3}{6} S \end{bmatrix} \tag{4}$$

III. ESTIMATION OF NOISE STATISTICS

The statistical model taken for the random (unmodeled) acceleration vector u in Ref [1] is of the form

$$u(k+1) = u(k) + \dot{u}(k)\tau, \quad \tau = t_{k+1} - t_k, \tag{5}$$

where

$$\dot{u}(k+1) = \dot{u}(k) \tag{6}$$

and the covariance matrix of $\dot{u}$ is specified a' priori to be some (diagonal) matrix $\bar{U}_{\dot{u}\dot{u}}$ which is not allowed to decrease as a result of the estimation process (as in a "consider" filter mode). On the other hand, u and $\dot{u}$ are estimated (unlike the "consider" filter mode). This is the basic J-Adaptive filter.

Specification of $\bar{U}$ in the above filter requires some engineering judgement and experimentation in a given problem, and has been found to be information rate dependent. It is clearly desirable to automate the process of selection of $\bar{U}$ by making it data dependent, or adaptive. Such adaptive estimation of $\bar{U}$ (or some other statistic in a random model for the acceleration u) is the subject of the present report.

The basic approach taken to the estimation of the statistics of the acceleration u is the adaptive filtering approach of Refs [3,4]. In essence, at each measurement time k, that value of the statistic is selected which produces the most likely average measurement residual. This adaptive process for the selection of the statistics of u will be made explicit below within the context of the J-Adaptive filter.

The statistical model ultimately selected for u is given by

$$u(k+1) = u(k) + \tau w(k) \tag{7}$$

where $\{w(k)\}$ is a 3-vector, zero-mean, white Gaussian sequence with identically distributed components and covariance matrix

$$\varepsilon\{w(k)w^T(\ell)\} = q(k)I\,\delta_{k\ell}\ , \tag{8}$$

where $q(k)$ is to be estimated from the measurements. The model for u given in Eqs (5-6) was abandoned in favor of the model given in Eqn (7) for the following reasons. The filter with the model in Eqs (5-6) contains correlation matrices $C_{\dot{u}}$ (correlation between the state and $\dot{u}$) and $U_{u\dot{u}}$ (correlation between u and $\dot{u}$). These correlation matrices force the state covariance matrix P and the u covariance matrix U_{uu}. $C_{\dot{u}}$ and $U_{u\dot{u}}$ are in turn forced by $\bar{U}_{\dot{u}\dot{u}}$. When $\bar{U}_{\dot{u}\dot{u}}$ fluctuates randomly, as it does when it is estimated from the measurements, it introduces numerical inaccuracies in the correlations $C_{\dot{u}}$ and $U_{u\dot{u}}$. These in turn cause ill-conditioning of P and U_{uu}, sometimes to the point of loss of positive definiteness.

The complete dynamical model selected is therefore given by

$$\begin{aligned} &x(k+1) = \phi_m(x(k),\ Su(t)),\quad u(t) = u(k) + (t-t_k)w(k) \\ &u(k+1) = u(k) + \tau w(k) \end{aligned} \tag{9}$$

where x is the state vector (R,V) and ϕ_m is the mapping defined by Eqn (2). The measurement model is given by

$$y_i(k) = h_i(x(k)) + v_i(k),\quad i = 1,N \tag{10}$$

where y_i are the scalar measurements available at time k, and $\{v_i(k)\}$ are independent, scalar, zero-mean, white Gaussian noise sequences with

$$\varepsilon\{v_i(k)v_i^T(\ell)\} = R_{ii}(k)\delta_{k\ell}\ . \tag{11}$$

The measurement model is written in vector form as

$$y(k) = h(x(k)) + v(k)\ , \tag{12}$$

where

$$y^T = [y_1 \cdots y_N],\quad h^T = [h_1 \cdots h_N],\quad R = \text{diag}\ (R_{ii}). \tag{13}$$

Now define the sensitivity matrices

$$\Phi(k+1,k) = \left[\frac{\partial x(k+1)}{\partial x(k)}\right] = \left[\frac{\partial \phi_m}{\partial x(k)}\right]$$

$$\Psi(k+1,k) = \left[\frac{\partial x(k+1)}{\partial u(k)}\right] \triangleq \begin{bmatrix} \frac{\tau^2}{2} & S \\ \tau & S \end{bmatrix} \tag{14}$$

$$\Gamma(k+1,k) = \left[\frac{\partial x(k+1)}{\partial w(k)}\right] \triangleq \begin{bmatrix} \frac{\tau^3}{6} & S \\ \frac{\tau^2}{2} & S \end{bmatrix}$$

$$M(k) = \begin{bmatrix} M_1(k) \\ \vdots \\ M_N(k) \end{bmatrix} = \left[\frac{\partial h(x(k))}{\partial x(k)}\right]$$

and the covariance and correlation matrices

$$\begin{aligned} P(k|\ell) &= \varepsilon\{[\underline{x}(k) - \hat{x}(k|\ell)]\ [\underline{x}(k) - \hat{x}(k|\ell)]^T\} \\ C_u(k|\ell) &= \varepsilon\{[\underline{x}(k) - \hat{x}(k|\ell)]\ [\underline{u}(k) - \hat{u}(k|\ell)]^T\} \\ U(k|\ell) &= \varepsilon\{[\underline{u}(k) - \hat{u}(k|\ell)]\ [\underline{u}(k) - \hat{u}(k|\ell)]^T\} \end{aligned} \tag{15}$$

where $P(k|\ell)$ is the state estimation error covariance matrix (covariance of errors in $\hat{x}(k|\ell)$) at time t_k, given all measurement up to and including time t_ℓ. C_u and U have similar meaning. Then the usual extended Kalman filter[4] with variance $q(k)$ known and specified is given below.

Prediction (in time) is given by

$$\begin{aligned} \hat{x}(k+1|k) &= \phi_m(\hat{x}(k|k), S\hat{u}(t|k)) \\ \hat{u}(k+1|k) &= \hat{u}(k|k) \end{aligned} \tag{16}$$

$$
\begin{aligned}
P'(k+1|k) &= \Phi P(k|k)\Phi^T + \Phi C_u(k|k)\Psi^T + \Psi C_u^T(k|k)\Phi^T + \Psi U(k|k)\Psi^T \\
P(k+1|k) &= P'(k+1|k) + q(k)\Gamma\Gamma^T \\
C_u(k+1|k) &= \Phi C_u(k|k) + \Psi U(k|k) + q(k)\tau\Gamma \\
U(k+1|k) &= U(k|k) + q(k)\tau^2 I
\end{aligned}
\tag{17}
$$

where the argument (k+1,k) has been omitted from the matrices Φ, Ψ and Γ. The (measurement) update is given by

$$
\begin{aligned}
\hat{x}(k|k) &= \hat{x}(k|k-1) + K_x(k)\left[y(k) - h(\hat{x}(k|k-1))\right] \\
\hat{u}(k|k) &= \hat{u}(k|k-1) + K_u(k)\left[y(k) - h(\hat{x}(k|k-1))\right]
\end{aligned}
\tag{18}
$$

$$
\begin{aligned}
P(k|k) &= P(k|k-1) - K_x(k)M(k)P(k|k-1) \\
C_u(k|k) &= C_u(k|k-1) - K_x(k)M(k)C_u(k|k-1) \\
U(k|k) &= U(k|k-1) - K_u(k)M(k)C_u(k|k-1)
\end{aligned}
\tag{19}
$$

where

$$
\begin{aligned}
K_x(k) &= P(k|k-1)M^T(k)Y^{-1}(k) \\
K_u(k) &= C_u^T(k|k-1)M^T(k)Y^{-1}(k)
\end{aligned}
\tag{20}
$$

and where

$$
Y(k) = M(k)P(k|k-1)M^T(k) + R(k) \tag{21}
$$

Now the variance $q(k)$ will be estimated via the techniques of Refs [3, 4]. To that end, define the average normalized predicted residual at time $k+1$,

$$\bar{r}_{k+1} = \frac{1}{N} \sum_{\ell=1}^{N} \frac{\left[y_\ell(k+1) - h_\ell(\hat{x}(k+1|k)) \right]}{R_{\ell\ell}^{\frac{1}{2}}(k+1)} \tag{22}$$

It is easy to compute

$$\varepsilon\{\bar{r}_{k+1}^2\} = \varepsilon\{\bar{r}_{k+1}^2 | q(k) \equiv 0\} + dq(k) \tag{23}$$

where

$$\varepsilon\{\bar{r}_{k+1}^2 | q(k) \equiv 0\} = \frac{1}{N} + \frac{1}{N^2} \sum_{\ell=1}^{N} \sum_{m=1}^{N} \frac{M_\ell(k+1) P'(k+1|k) M_m^T(k+1)}{R_{\ell\ell}^{\frac{1}{2}}(k+1)\, R_{mm}^{\frac{1}{2}}(k+1)} \tag{24}$$

$$d = \frac{1}{N^2} \sum_{\ell=1}^{N} \sum_{m=1}^{N} \frac{M_\ell(k+1) \Gamma \Gamma^T M_m^T(k+1)}{R_{\ell\ell}^{\frac{1}{2}}(k+1)\, R_m^{\frac{1}{2}}(k+1)} \tag{25}$$

Then the most probable $q(k)$ based on $\bar{r}_{k+1}$ is given by [3,4]

$$\bar{q}(k) = \begin{cases} \frac{1}{d} \left[\bar{r}_{k+1}^2 - \alpha \varepsilon\{ \bar{r}_{k+1}^2 | q(k) \equiv 0 \} \right], & \text{if positive} \\ 0 , & \text{otherwise} \end{cases} \tag{26}$$

with $\alpha = 1$.

The estimate $\hat{q}(k)$ of $q(k)$ utilized is an exponentially age-weighted average of $\bar{q}(k)$ generated from

$$\begin{aligned} c_k &= a c_{k-1} + 1, \quad c_{-1} = 0, \quad a < 1, \\ \hat{q}(k) &= \frac{c_k - 1}{c_k} \hat{q}(k-1) + \frac{1}{c_k} \bar{q}(k), \quad \hat{q}(-1) = 0 . \end{aligned} \tag{27}$$

The $\hat{q}(k)$ from Eqs (27) is used for $q(k)$ in the filter equations (17).

To complete the estimator equations, the symmetry matrix S in Eqs (14) and (16) must be specified. A matrix S used with success is given by

$$S(k) = \frac{1}{|\hat{R}(k|k)|} \begin{bmatrix} -\hat{x}(k|k) & 0 & 0 \\ 0 & -\hat{y}(k|k) & 0 \\ 0 & 0 & -\hat{z}(k|k) \end{bmatrix} \tag{28}$$

This points the acceleration vector u at the center of the earth.

IV. DETAILS OF SIMULATIONS

The simulations presented in the next section feature a circular, polar orbit of approximately 1000 km altitude. The "real" system force model consists of the two-body model, plus the earth oblateness model given in Appendix A, plus a mascon (mass concentration) buried at a depth of 100 km. The mascon acceleration is represented as

$$\ddot{\Delta R}_m = -\mu_m \left[\frac{R - R_m}{|R - R_m|^3} + \frac{R_m}{|R_m|^3} \right] \tag{29}$$

where R is of course the satellite position vector, R_m is the mascon position vector, and $\mu_m = 0.02\ km^3/sec^2$ [so that $\mu_m \approx 5 \times 10^{-8} \mu$, where μ is the gravitational parameter of the earth]. In summary, the real system is represented by

$$\ddot{R} = -\frac{\mu R}{r^3} + \ddot{\Delta R}_o + \ddot{\Delta R}_m \tag{30}$$

To complete the specification of the system constants (see Appendix A), the rotation rate of the earth and the eccentricity of the earth are, respectively,

$$\omega = 7.2921159 \times 10^{-5}\ rad/sec, \quad e = 0.081813336\ . \tag{31}$$

Tracking (range and range rate) is simulated from several tracking stations to give continuous, and often overlapping, station coverage, sampled every 5 sec. Tracking begins at the north pole and usually continues for 50 minutes, which is slightly less than one-half the orbital period. The error models for range and range rate measurements are simplified, consisting only of additive white Gaussian noise. Measurement noise standard deviations vary, and are specified for each simulation.

Estimator dynamical models are variously two-body, and two-body plus approximate J_2 and J_3 oblateness accelerations. Precise estimator models used are specified in each simulation.

V. SIMULATION RESULTS

The first set of simulations to be described feature the J-Adaptive estimator with estimated noise variance q (J-A-$\hat{q}$ estimator) with a two-body dynamical model. The J-A-$\hat{q}$ estimator is also compared with the J-Adaptive estimator with engineered a priori statistic $\bar{U}_{\dot{u}\dot{u}}$ (J-A-$\bar{U}$ estimator), also with a two-body dynamical model. Note that, with a two-body model, closed form prediction equations are available, and no numerical integration is required.

Figures 1-7 show the performance of the J-A-$\hat{q}$ estimator with a two-body dynamical model, when the measurement noise standard deviations for range and range rate are $\sigma_\rho = 3$m, $\sigma_{\dot{\rho}} = 1$ cm/sec, respectively. As indicated in Section IV, continuous and often overlapping tracking station coverage is available. Figures 1-3 show the tracking of the unmodeled acceleration. The solid lines represent the actual unmodeled acceleration (oblateness and mascon), while the dots are the estimates $S\hat{u}$. The z-component of the unmodeled acceleration dominates, being of the order of 10^{-5} (initally 10^{-4}) km/sec^2, and is therefore tracked most precisely. The x and y acceleration component estimates are more noisy, but are clearly tracked. Note that there is an initial transient lasting about 300 sec or so before the J-A-$\hat{q}$ estimator locks onto the unmodeled acceleration. Figures 4 and 5 show the normalized measurement residuals (normalized by their noise standard deviations) for range and range rate. The initial transient described above exhibits itself in the range rate residuals, producing initially, rather large residuals. This transient dies out, however, and the measurement residuals then appear quite white and are within the measurement noise level. The absence of residuals after about 2000 sec of tracking is merely a programming problem in the computer-generated plots; the residuals continue to exhibit appropriate statistical properties for the balance of 1000 sec. Figures 6 and 7 show the actual state estimation errors in position and velocity; namely $|R-\hat{R}|$ and $|V-\hat{V}|$. It is seen that after an initial transient the state estimation errors are quite comparable with the measurement noise. That is, position is estimated to about 3m and velocity to about 1-5 cm/sec.

Let us discuss the initial ~ 300 sec transient which is observed in Figures 1-7. This transient is, in part, due to the transient in $\hat{u}$; that is,

the state cannot be estimated precisely until the unmodeled acceleration is. This is not the whole story, however, Note that the range rate normalized residuals, while sometimes as large as 5σ initially, are random and cannot explain the large initial state estimation errors, particularly in velocity. It is noted that the drop in state errors at about 300 sec coincides with acquisition of the satellite by a second tracking station. It is also noted that the position and velocity estimation errors are largely in the x and y components; the z component errors are quire small. This is simply due to the station-satellite geometry. Thus from the first station, x, y, $\dot{x}$ and $\dot{y}$ are not as observable as z and $\dot{z}$ are. This geometric observability clearly has an impact on the estimation of Su as well; and also on the estimation of $\hat{q}$. $\hat{q}$ guarantees residuals consistent with a projection of the state covariance matrix on the *available* measurement space; not on the unobservable subspace of state space. This last observation was well evidenced in a simulation with range rate measurements only. In that case, range rate residuals were just as nice as in the present simulation, while state errors were not quite as good during the first 300 sec of tracking. $\hat{q}$ compensated only for the state subspace it could see. This leads to the observation that while additional measurement types (e.g. angles) may not enhance a standard estimation process (e.g. batch), they may well enhance the J-A-$\hat{q}$ estimator.

The precision of tracking of the unmodeled acceleration can be improved with more precise measurements. This can be seen in Figure 8, which shows the x acceleration component estimate generated by the J-A-$\hat{q}$ estimator with σ_ρ = 0.3m and $\sigma_{\dot{\rho}}$ = 0.1 cm/sec. Compare this with Figure 1.

The J-A-$\bar{U}$ estimator was simulated on the case described above (σ_ρ = 3m, $\sigma_{\dot{\rho}}$ = 1 cm/sec). This was easy to do once the J-A-$\hat{q}$ run was made; $\bar{U}$ was set at the steady-state value of $\hat{q}I$. Figure 9 shows the tracking of the x acceleration component. Comparing this with Figure 1, improvement in tracking is seen, although the J-A-$\bar{U}$ estimates definitely have deterministic oscillations and are not as desirable from this point of view. Figure 10 shows that the J-A-$\bar{U}$ estimator produces somewhat nicer measurement residuals than the J-A-$\hat{q}$ estimator (compare with Figure 5). But a stand-alone J-A-$\bar{U}$ run would require

engineering the $\bar{U}$ statistics which would normally take several simulations. In contrast to this, all J-A-$\hat{q}$ estimator runs are completely automatic, and are *untouched by human hand.*

The next set of simulations to be described feature the J-A-$\hat{q}$ estimator with an improved dynamical model. In addition to the two-body term, the estimator contains the J_2 and J_3 terms with approximate values of J_2 and J_3; namely, $J_2 = 1.083 \times 10^{-3} R_E^2$, $J_3 = -2.55 \times 10^{-6} R_E^3$. The objective of these simulations is to determine how well the estimator might identify the higher order geopotential. Figure 11 shows the tracking of the z acceleration component with $\sigma_\rho = 3m$, $\sigma_{\dot{\rho}} = 1$ cm/sec. It is observed that the lower acceleration levels cannot be tracked with such noisy measurements. However, Figures 12 and 13 show that the state is still estimated to the data precision; the undetected accelerations are inconsequential relative to the overall noise levels. Figure 14 shows the tracking of the z acceleration component with $\sigma_\rho = 0.3m$, $\sigma_{\dot{\rho}} = 0.1$ cm/sec. Tracking is improved (compare with Figure 11), but the extremely low unmodeled accelerations are still undetected. Things of course look much better on a linear scale (see Figure 15). Tracking can be further improved with $\sigma_\rho = 3$ cm, $\sigma_{\dot{\rho}} = 0.01$ cm/sec, as can be seen in Figure 16. When better instruments are developed we will show additional simulations.

The next simulations feature an unmodeled mascon. That is, the only model error is due to the mascon. As seen in Figure 17, the J-A-$\hat{q}$ estimator (unaided by human hand) cannot track this extremely small unmodeled mascon acceleration. As can be seen in Figure 18, however, a carefully engineered J-A-$\bar{U}$ estimator does detect the mascon, albeit with some lag and overshoot which eventually damps out. To accomplish this, however, we need $\sigma_\rho = 1$ cm and $\sigma_{\dot{\rho}} = 0.01$ cm/sec.

Limited simulations were performed on a single station pass. This is the first station of the earlier simulations (recall the earlier station-satellite geometry discussion). The measurement noise standard deviations for range and range rate are $\sigma_\rho = 3m$, $\sigma_{\dot{\rho}} = 1$ cm/sec, respectively. Table 1 summarizes the position and velocity errors at the end of the pass for several cases. First a standard extended Kalman filter[4] run was made, where the filter model was perfect (full oblateness). The lack of good observability in the x and y

coordinate directions is clearly seen in Table 1 (although it should be noted that the filter was not iterated,[4] either locally or globally; some small improvement might be expected with iteration.) Next a totally uncompensated, standard extended Kalman filter run was made, where the filter model contained the two-body term and the J_2 and J_3 terms with the approximate values of J_2 and J_3 used above. It is seen in Table 1 that this uncompensated filter is diverging, as expected. A J-A-$\hat{q}$ estimator, with the two-body and the same approximate J_2 and J_3 terms was completely unsuccessful (started to diverge). This is due to the initial transient, discussed earlier, where the $\hat{u}$ estimates are poor; the J-A-$\hat{q}$ estimator is not yet locked onto the unmodeled acceleration. However, improved results are obtained (shown in the last line of Table 1), when the estimated $\hat{u}$ is not used for prediction. This might be termed an "adaptive consider mode" of the estimator. As seen in Table 1, these results (third line) are comparable to the perfect model run (first line) in the x and y coordinate directions. z-coordinate errors are larger, however; the J-A-$\hat{q}$ adaptive consider mode filter is putting too much uncertainty in the z-direction.

These single station pass simulations indicate that when observability is marginal, automatic adaptive estimation is of questionable value. Great care must be exercise in adding uncertainty to a selected subspace of the state space; so as not to destroy the information content of the data.

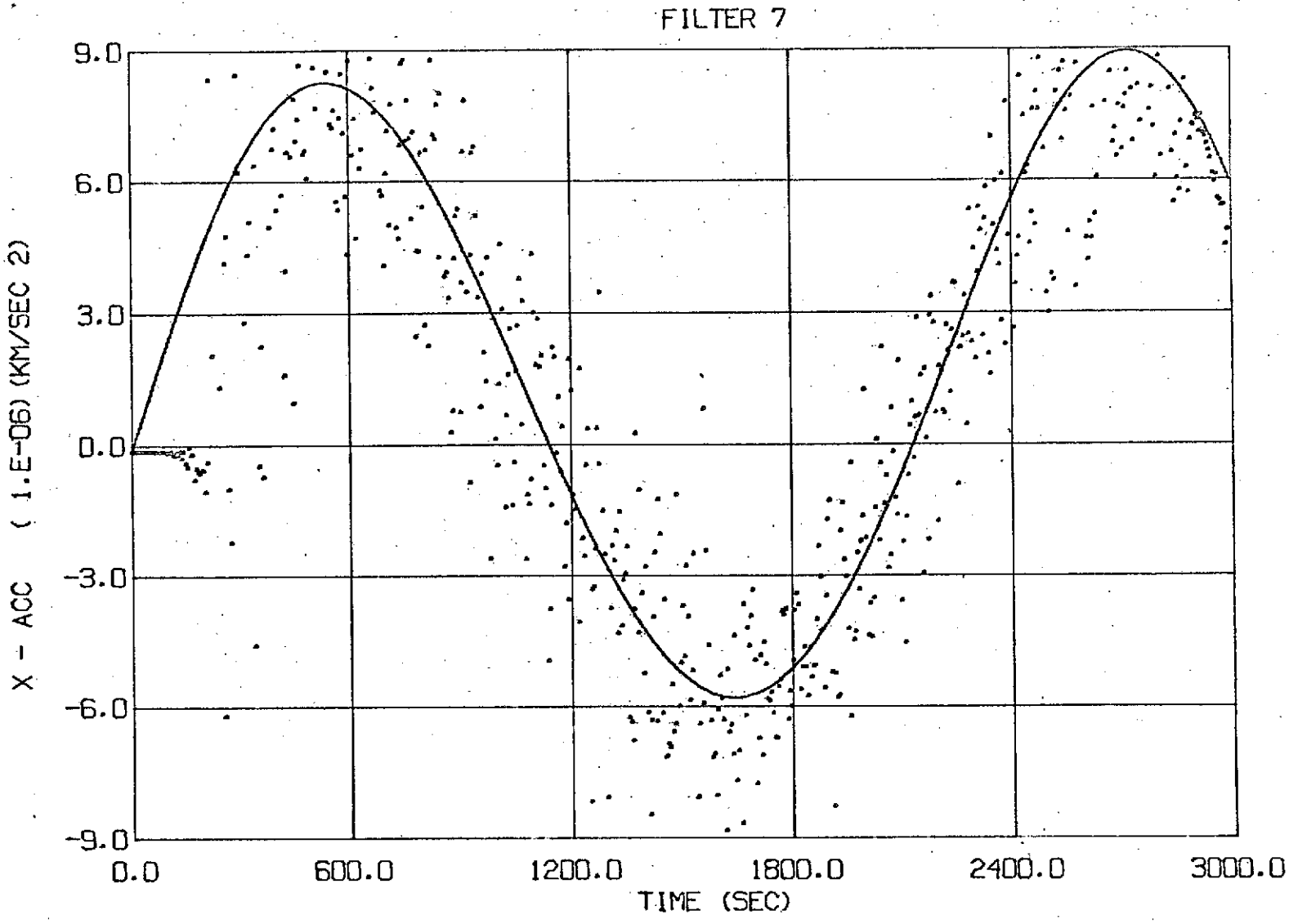

Figure 1. TRACKING THE x-ACCELERATION

($\hat{q}$; 2-body model; σ_ρ = 3m, $\sigma_{\dot\rho}$ = 1 cm/sec)

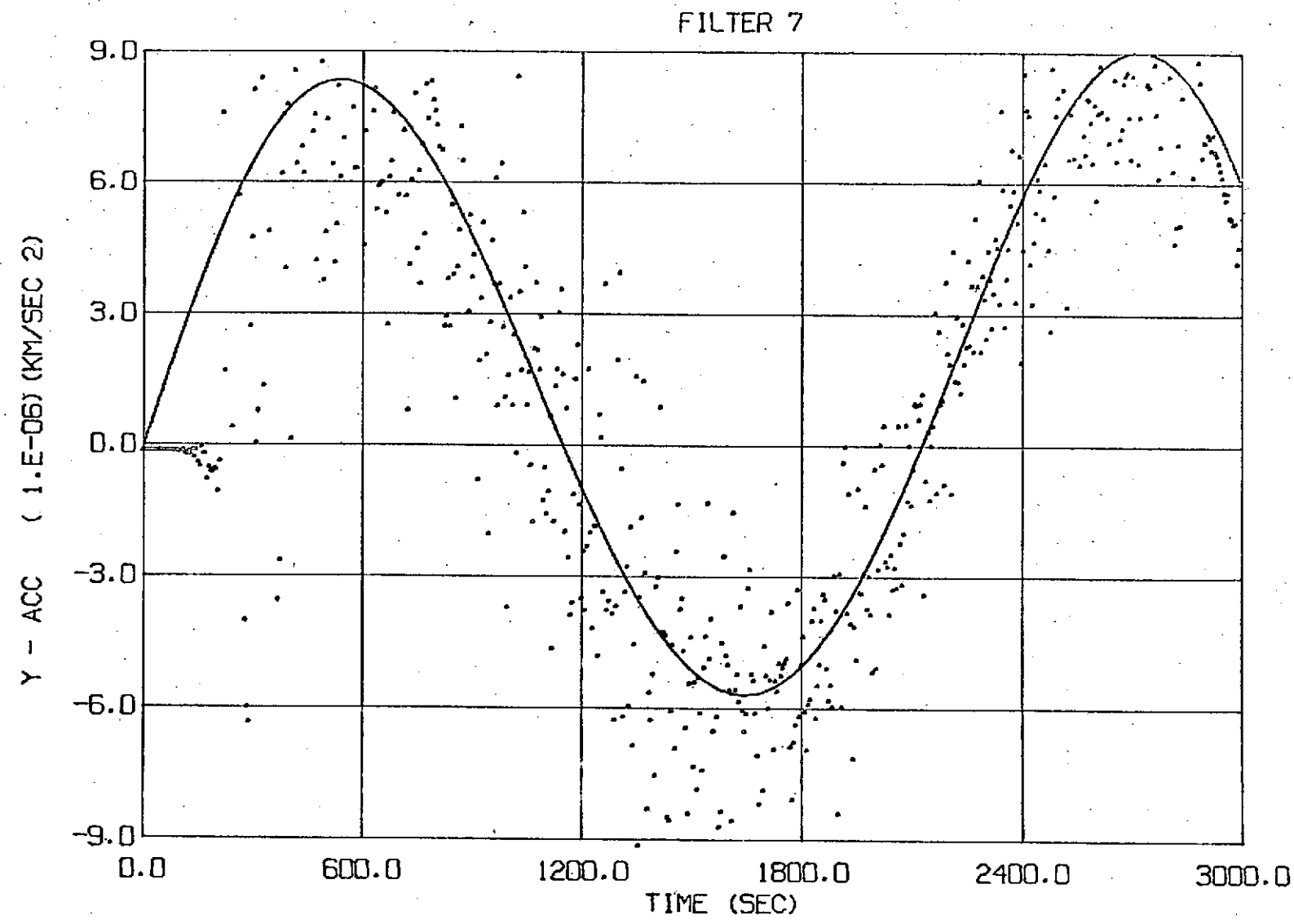

Figure 2. TRACKING THE y-ACCELERATION

($\hat{q}$; 2-body model; σ_ρ = 3m, $\sigma_{\dot{\rho}}$ = 1 cm/sec)

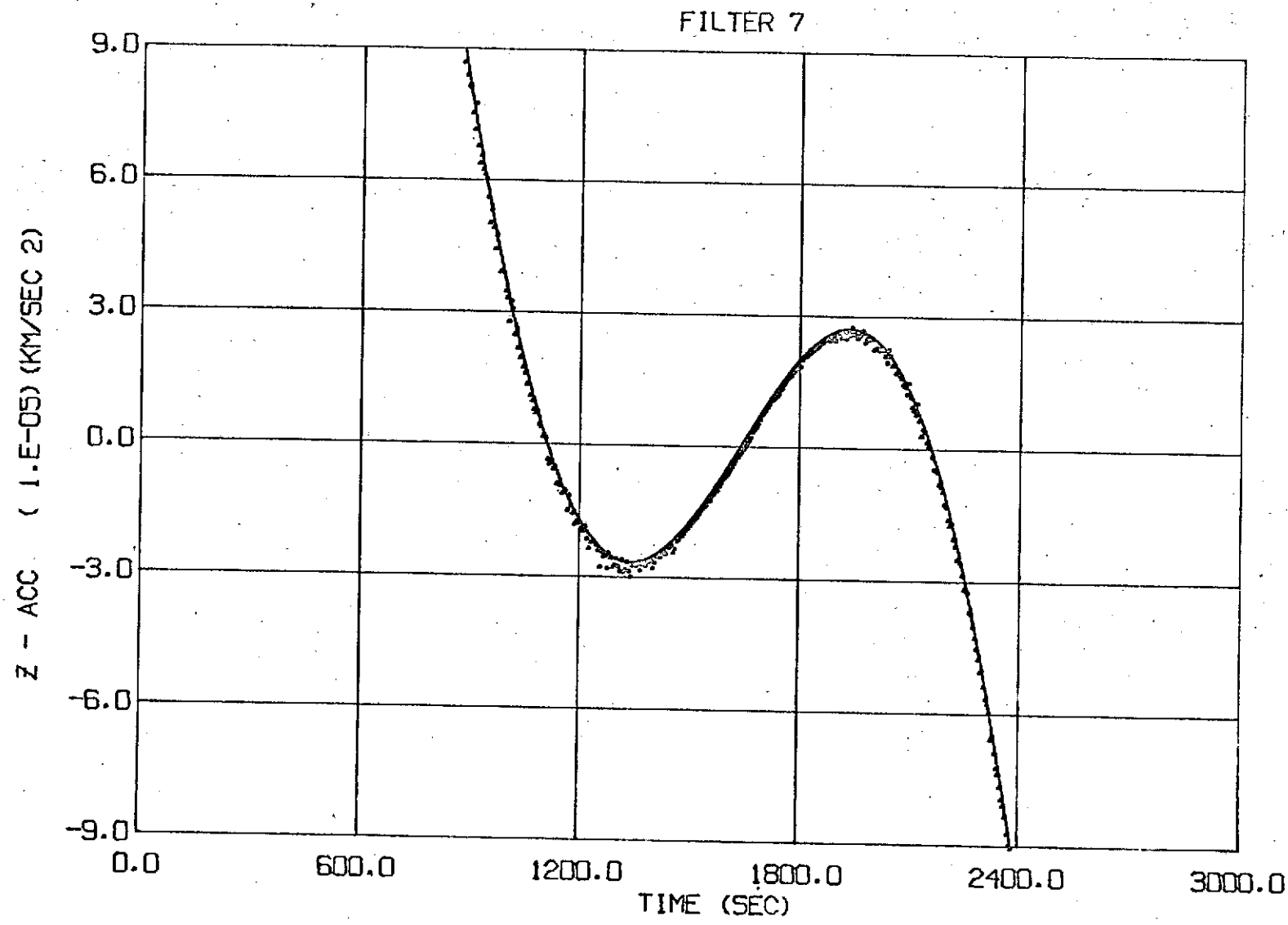

Figure 3. TRACKING THE z-ACCELERATION

($\hat{q}$; 2-body model; σ_ρ = 3m, $\sigma_{\dot{\rho}}$ = 1 cm/sec)

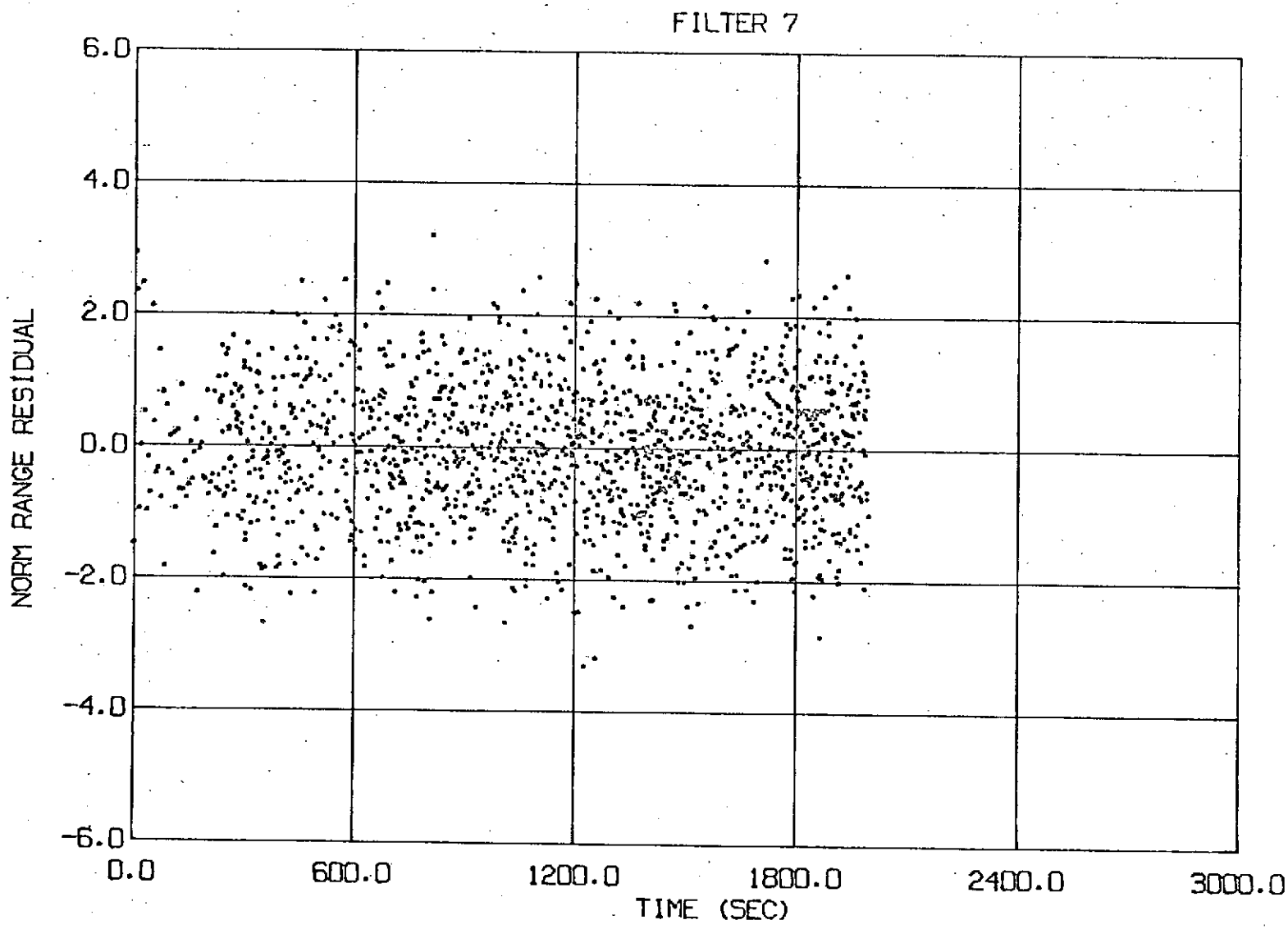

Figure 4. NORMALIZED RANGE RESIDUALS

($\hat{q}$; 2-body model; σ_ρ = 3m, $\sigma_{\dot{\rho}}$ = 1 cm/sec)

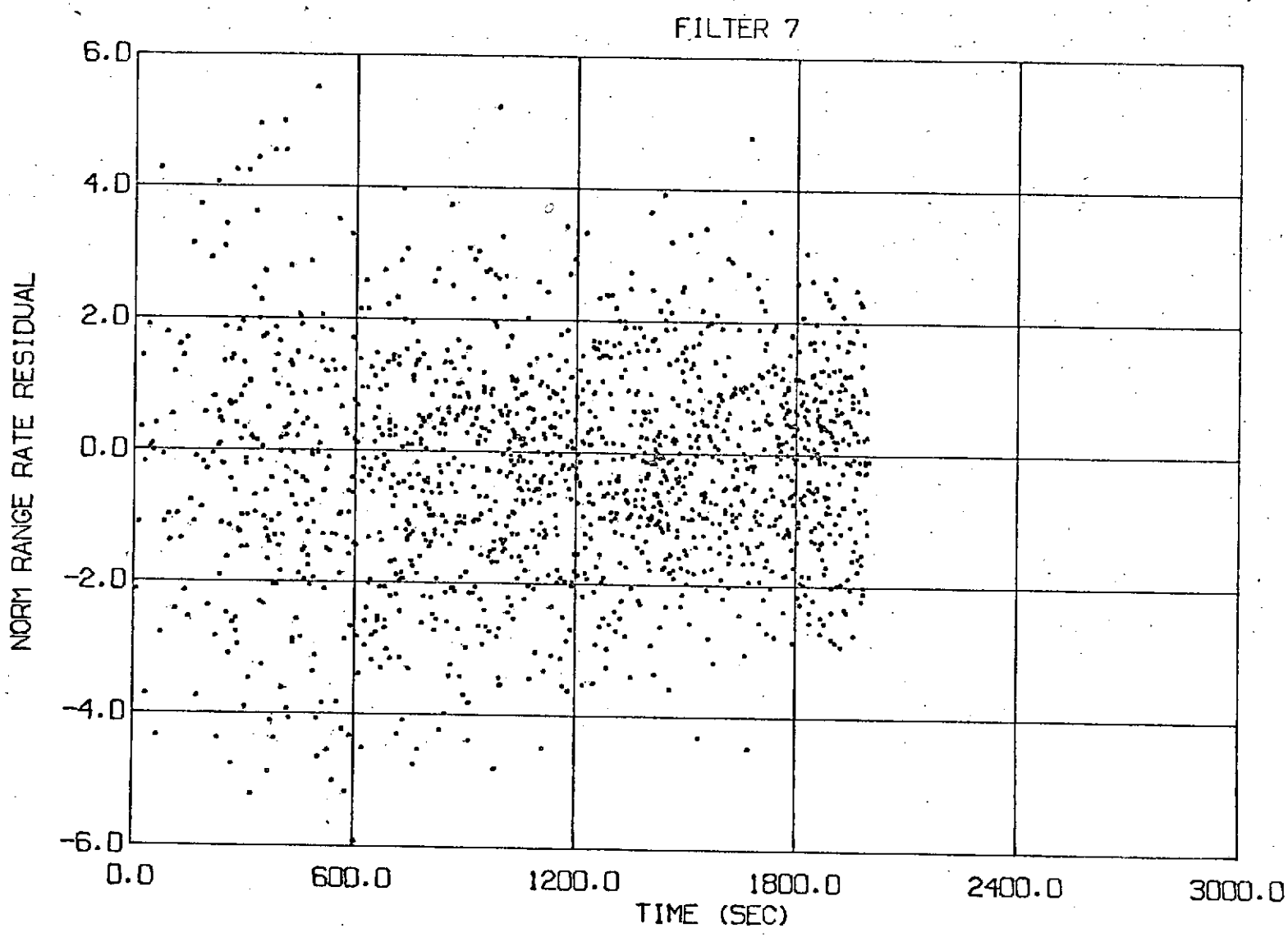

Figure 5. NORMALIZED RANGE RATE RESIDUALS

($\hat{q}$; 2-body model; σ_ρ = 3m, $\sigma_{\dot\rho}$ = 1 cm/sec)

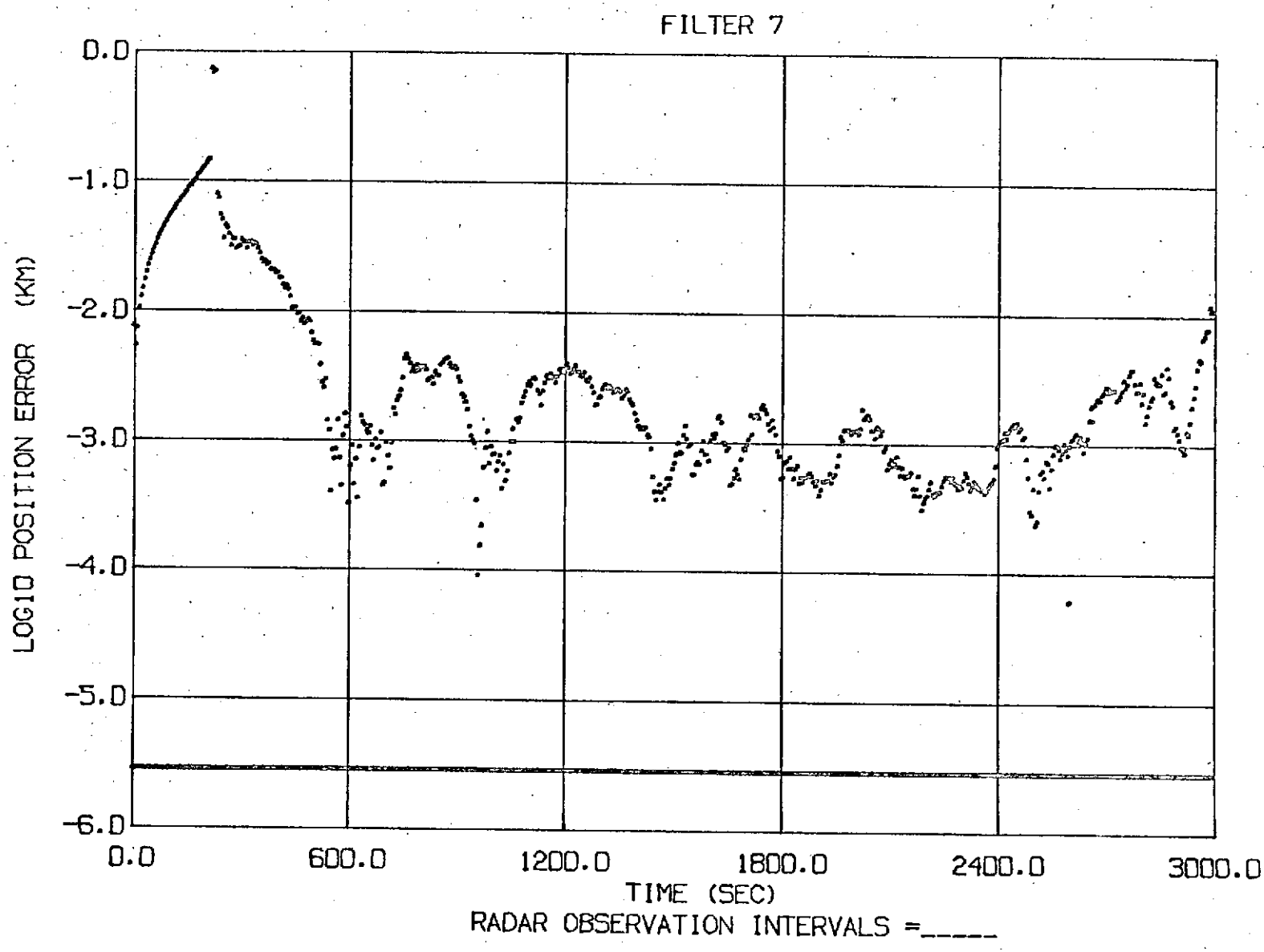

Figure 6. POSITION ESTIMATION ERRORS

($\hat{q}$; 2-body model; σ_ρ = 3m, $\sigma_{\dot{\rho}}$ = 1 cm/sec)

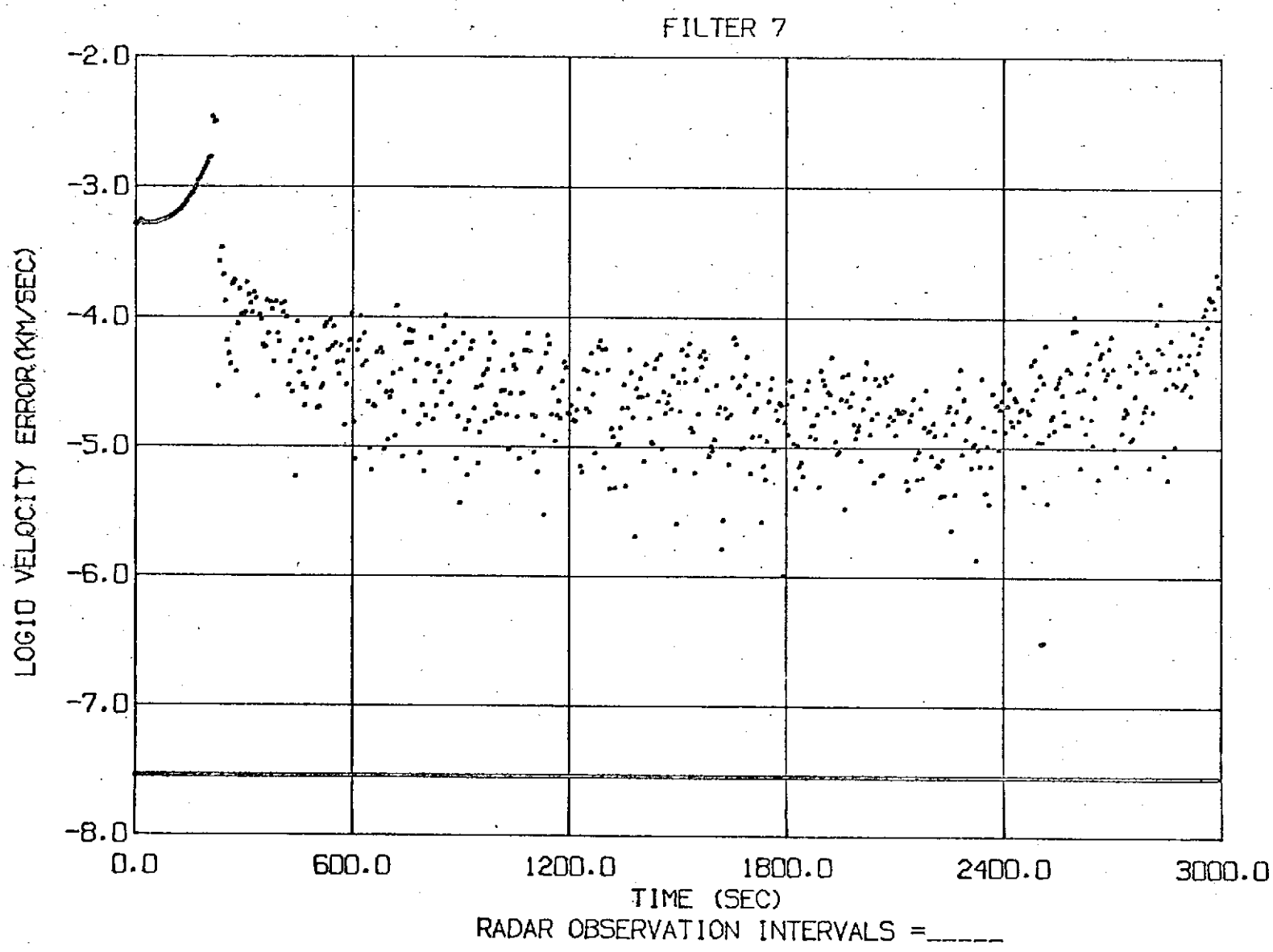

Figure 7. VELOCITY ESTIMATION ERRORS

($\hat{q}$; 2-body model; σ_ρ = 3m, $\sigma_{\dot{\rho}}$ = 1 cm/sec)

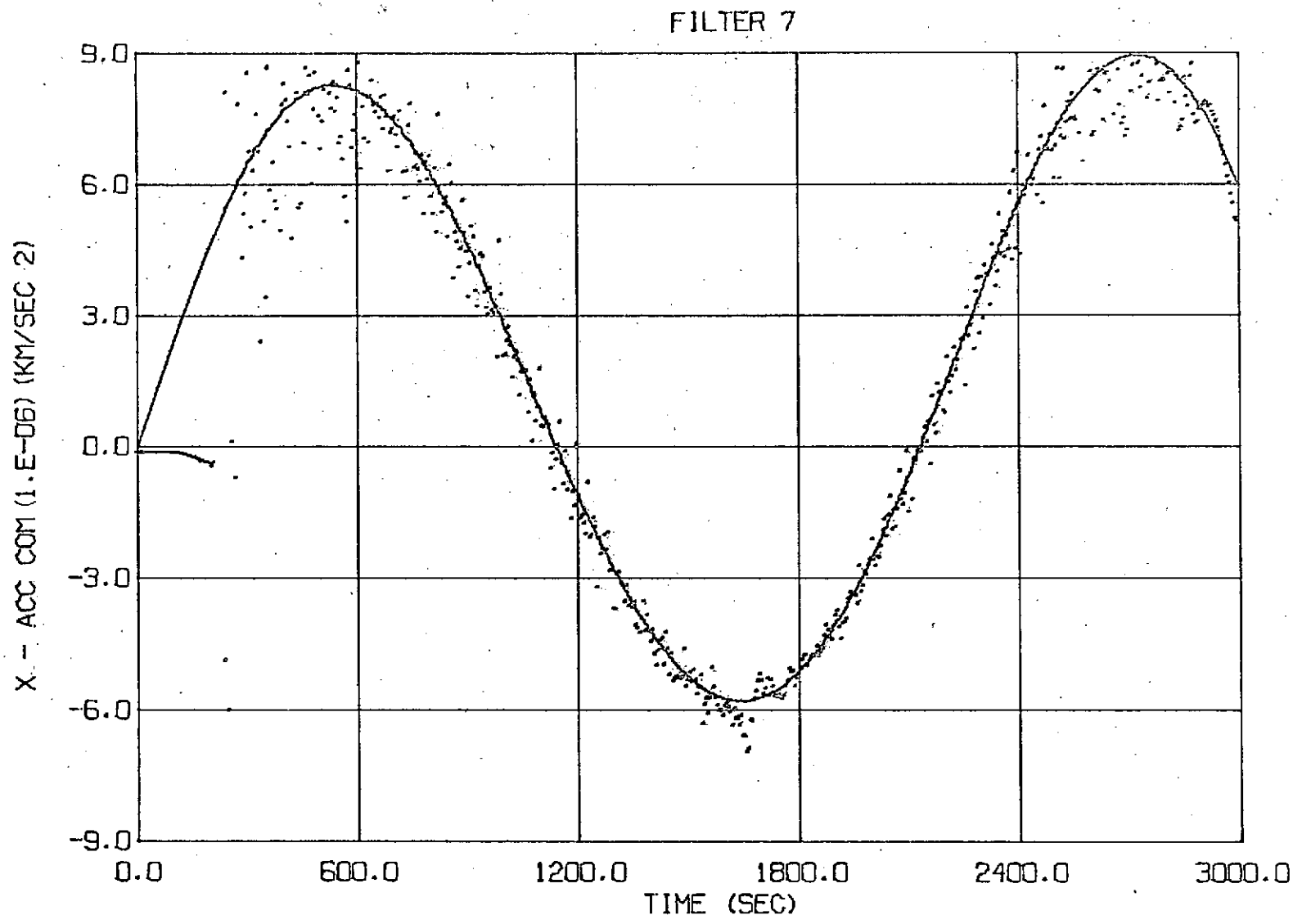

Figure 8. TRACKING THE x-ACCELERATION

($\hat{q}$; 2-body model; σ_ρ = 0.3m, $\sigma_{\dot{\rho}}$ = 0.1 cm/sec)

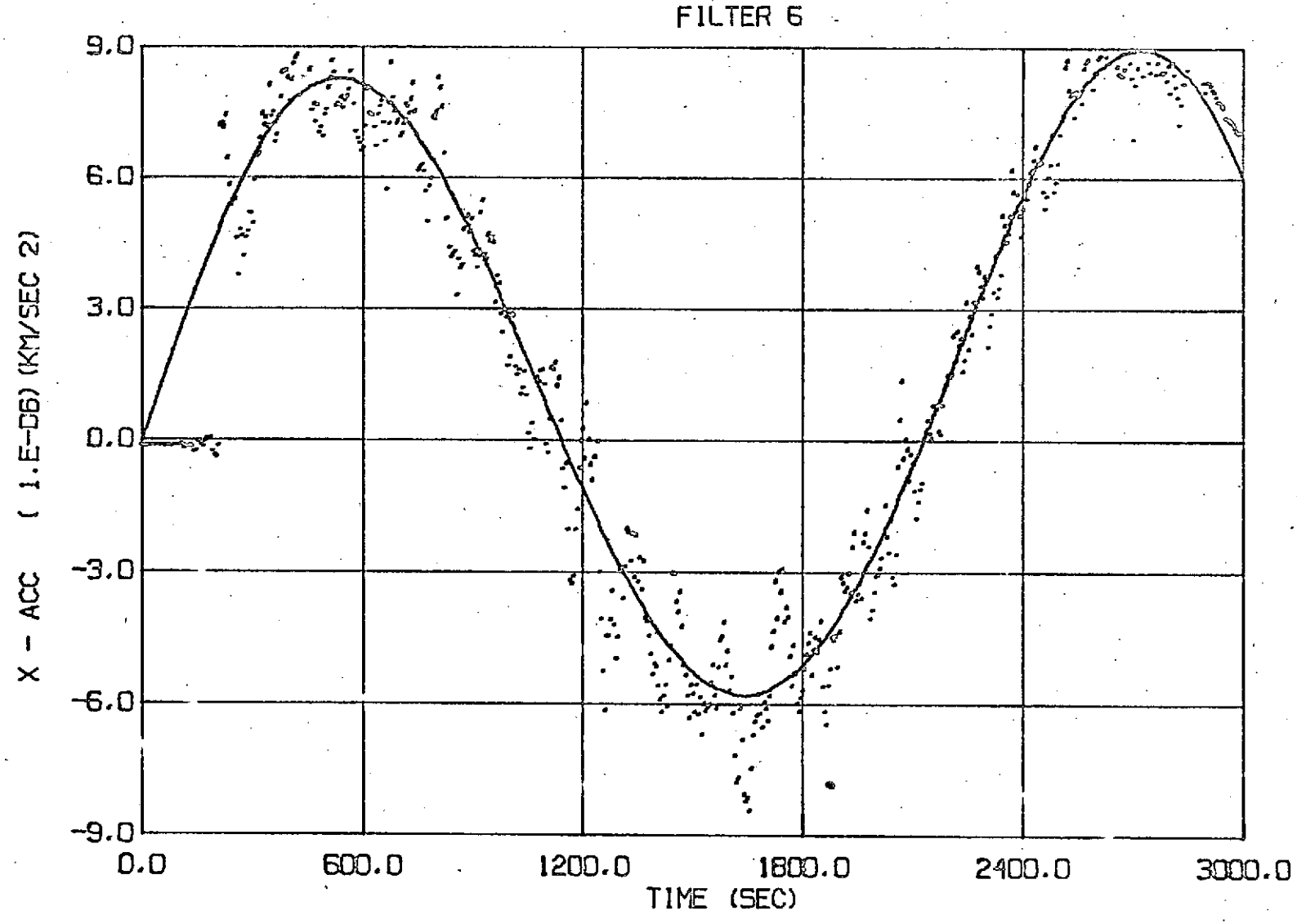

Figure 9. TRACKING THE x-ACCELERATION

($\bar{U}$; 2-body model; σ_ρ = 3m, $\sigma_{\dot{\rho}}$ = 1 cm/sec)

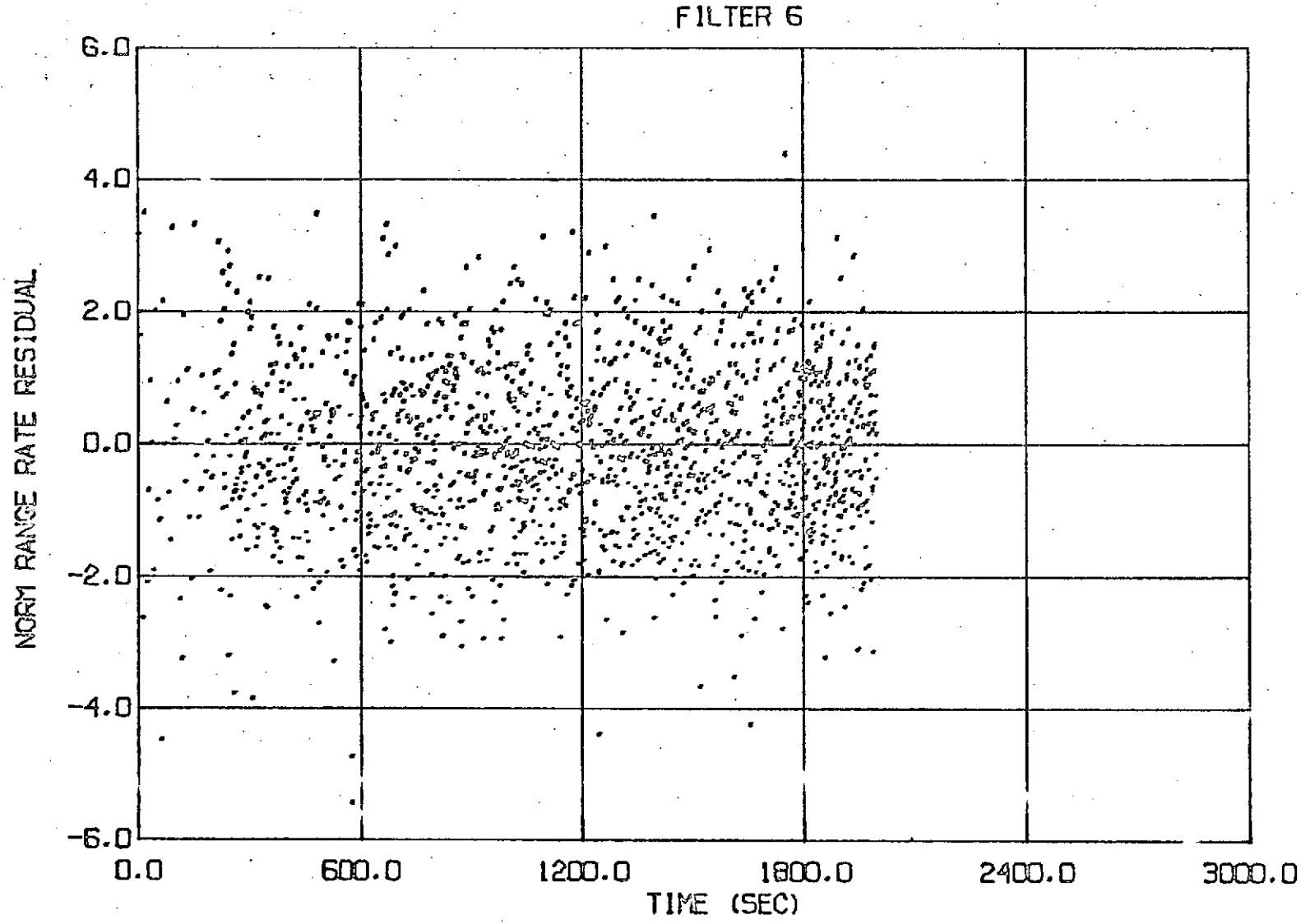

Figure 10. NORMALIZED RANGE RATE RESIDUALS
($\bar{U}$; 2-body model; σ_ρ = 3m, $\sigma_{\dot\rho}$ = 1 cm/sec)

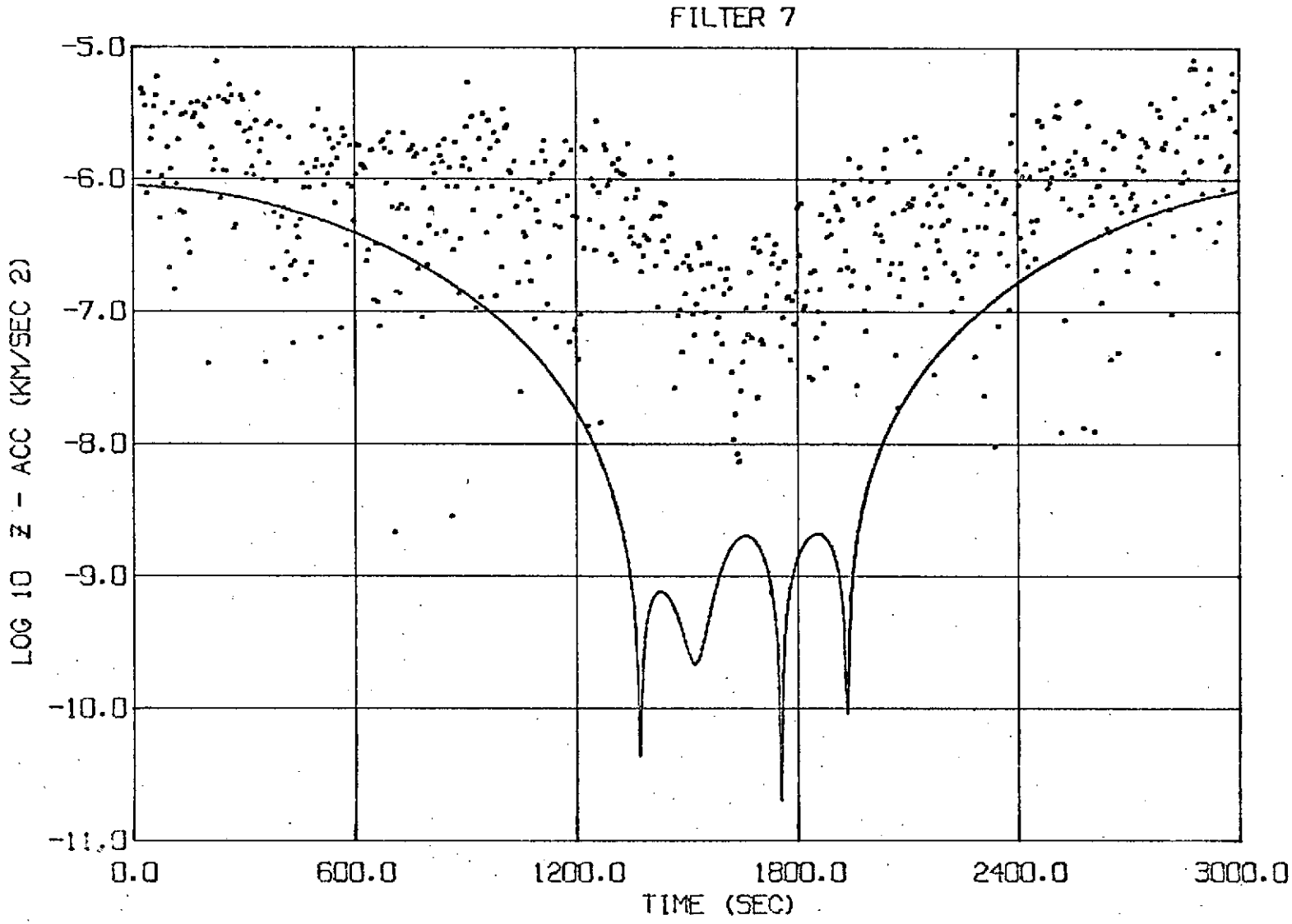

Figure 11. TRACKING THE z-ACCELERATION - LOG SCALE
($\hat{q}$; J_2, J_3 model; σ_ρ = 3m, $\sigma_{\dot{\rho}}$ = 1 cm/sec)

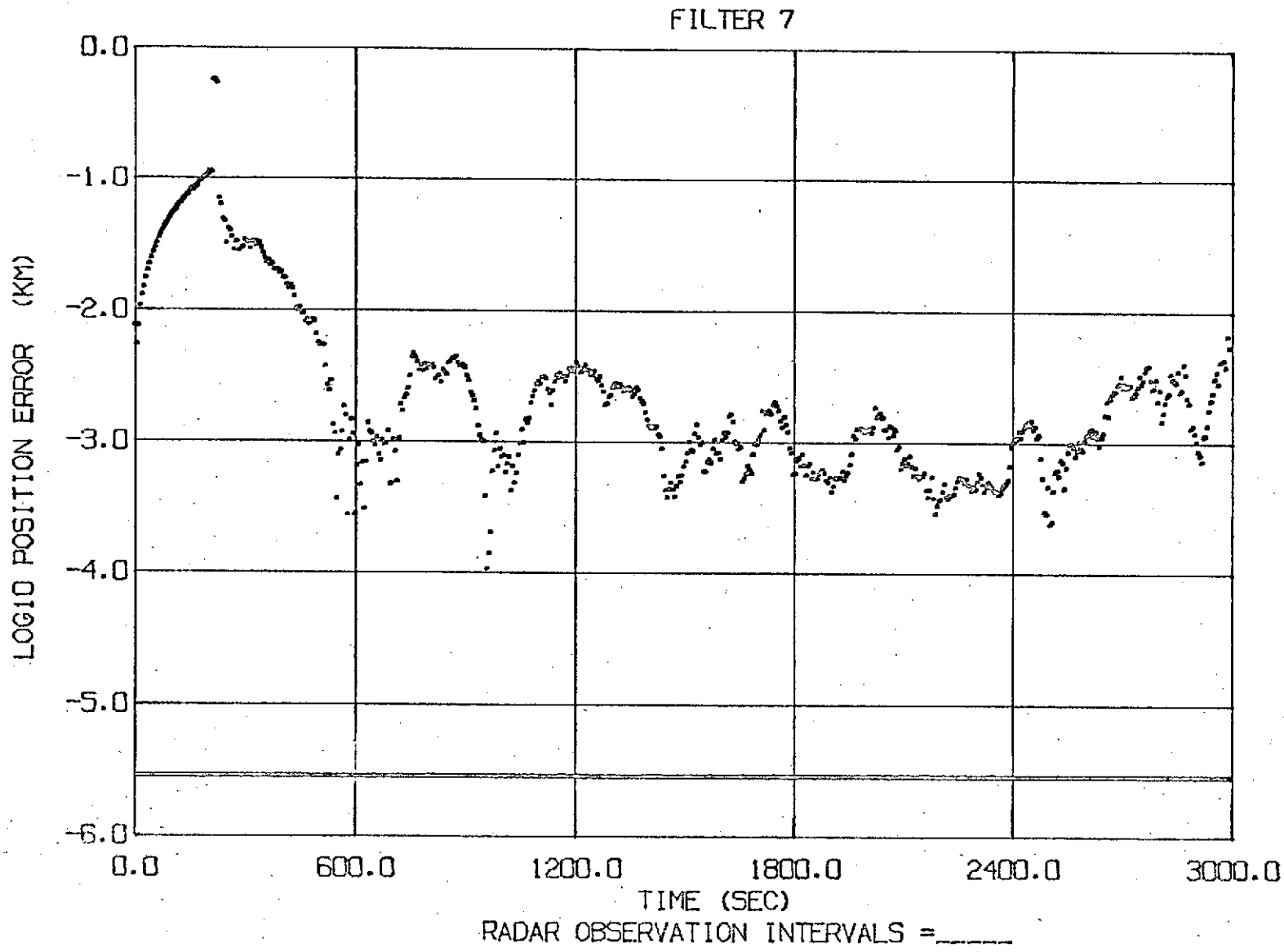

Figure 12. POSITION ESTIMATION ERRORS

($\hat{q}$; J_2, J_3 model; σ_ρ = 3m, $\sigma_{\dot{\rho}}$ = 1 cm/sec)

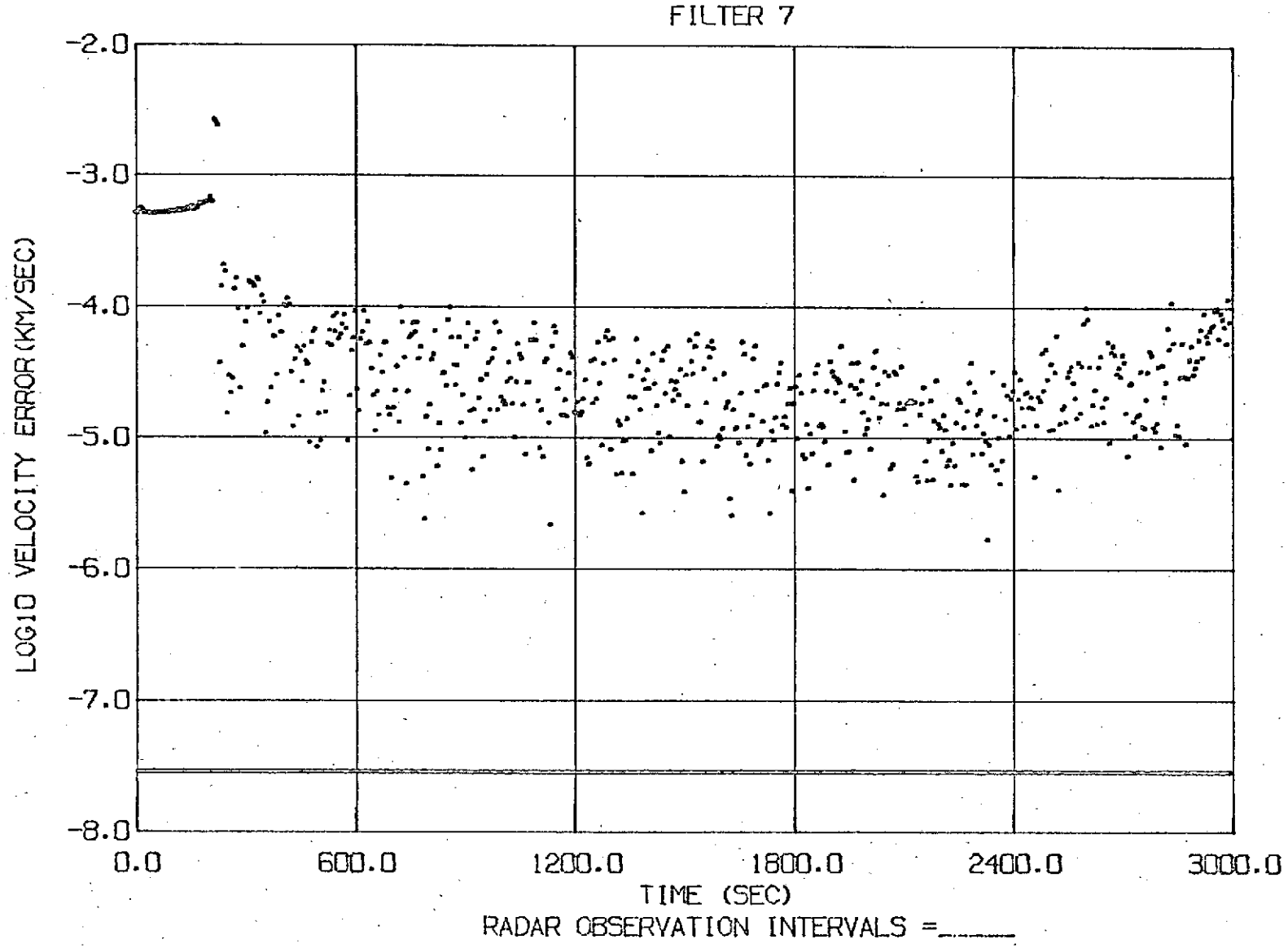

Figure 13. VELOCITY ESTIMATION ERRORS

($\hat{q}$; J_2, J_3 model; σ_ρ = 3m, $\sigma_{\dot{\rho}}$ = 1 cm/sec)

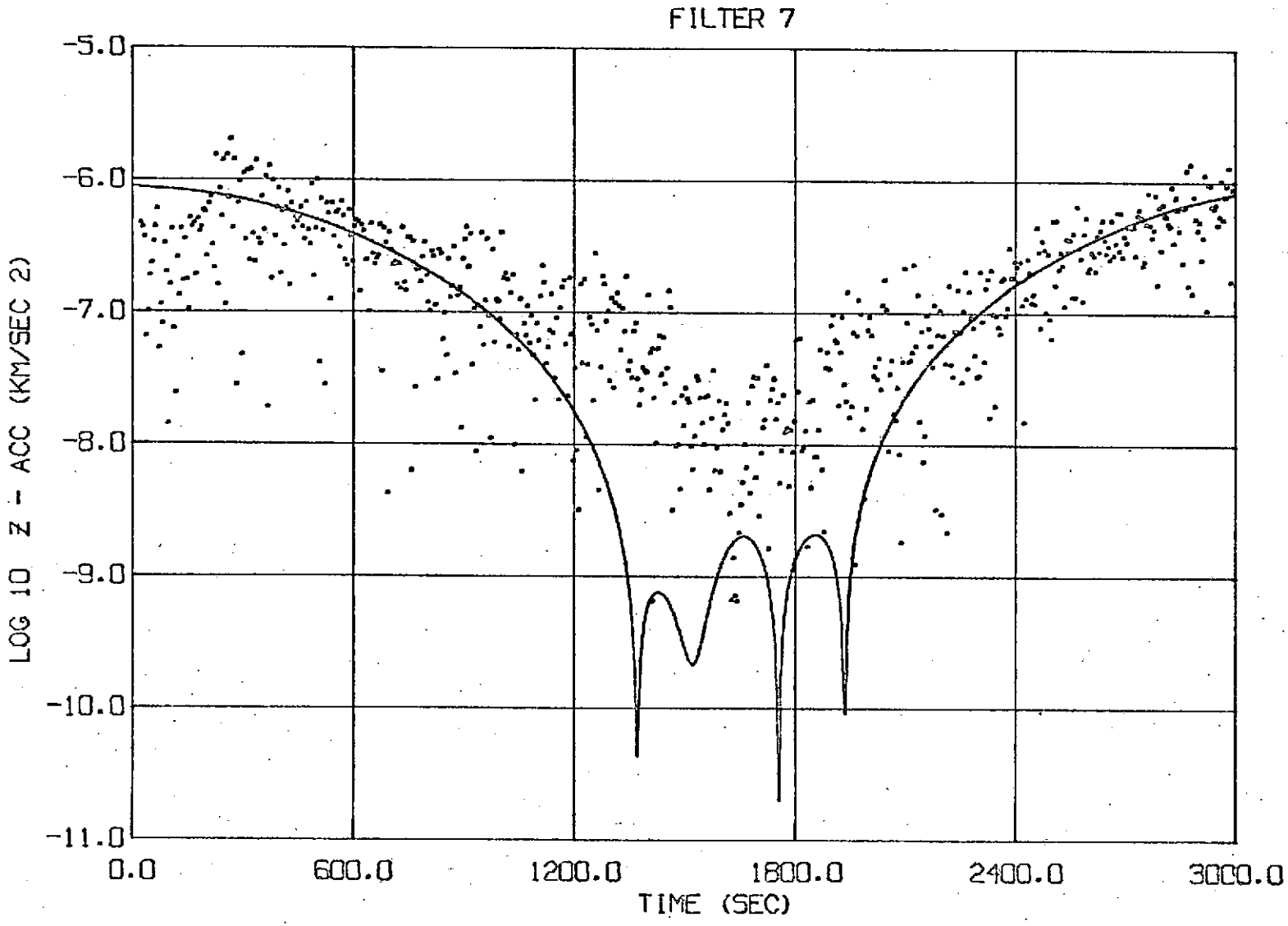

Figure 14. TRACKING THE z-ACCELERATION - LOG SCALE

($\hat{q}$; J_2, J_3 model; σ_ρ = 0.3m, $\sigma_{\dot{\rho}}$ = 0.1 cm/sec)

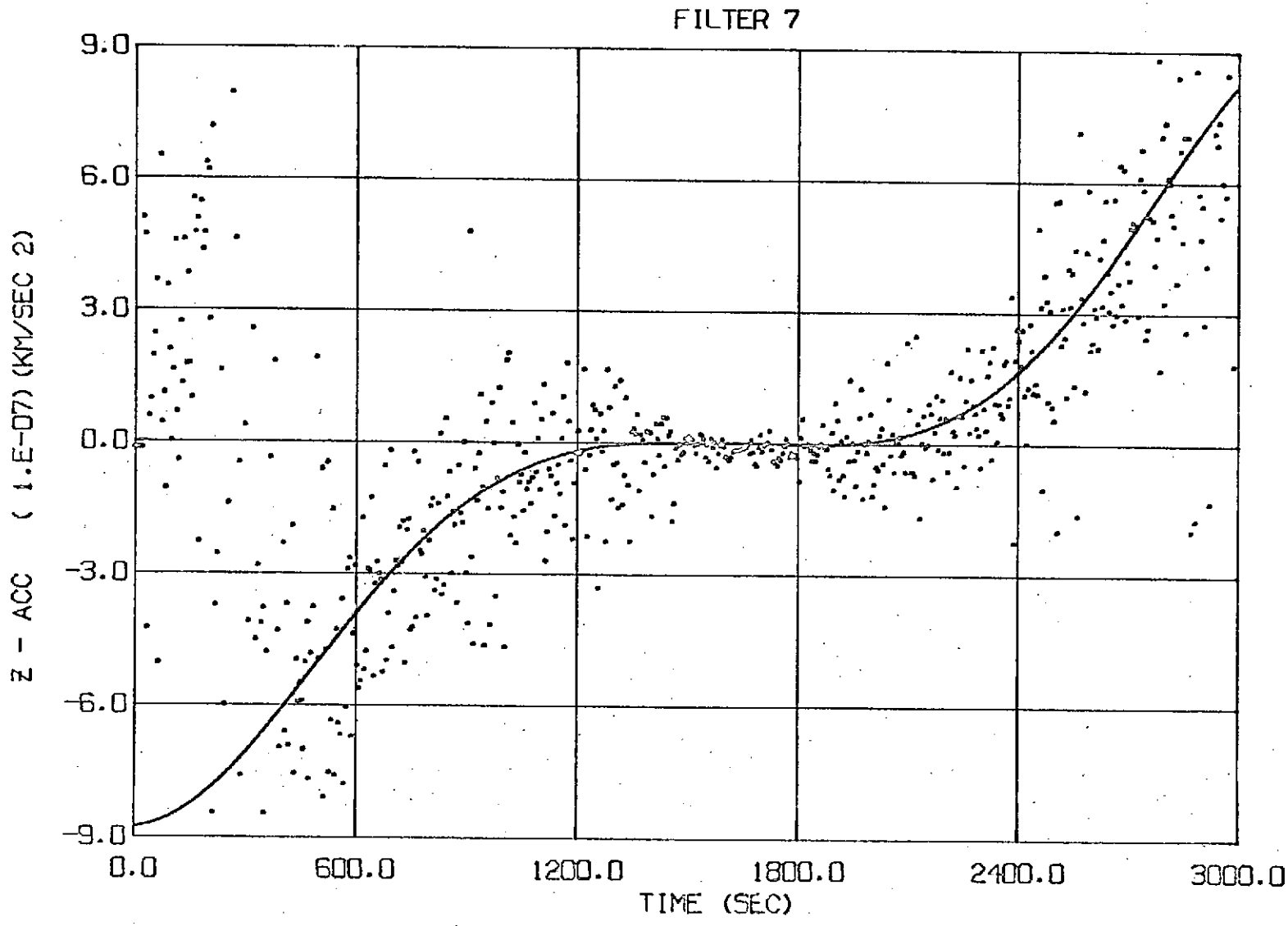

Figure 15. TRACKING THE z-ACCELERATION
($\hat{q}$; J_2, J_3 model; σ_ρ = 0.3m, $\sigma_{\dot{\rho}}$ = 0.1 cm/sec)

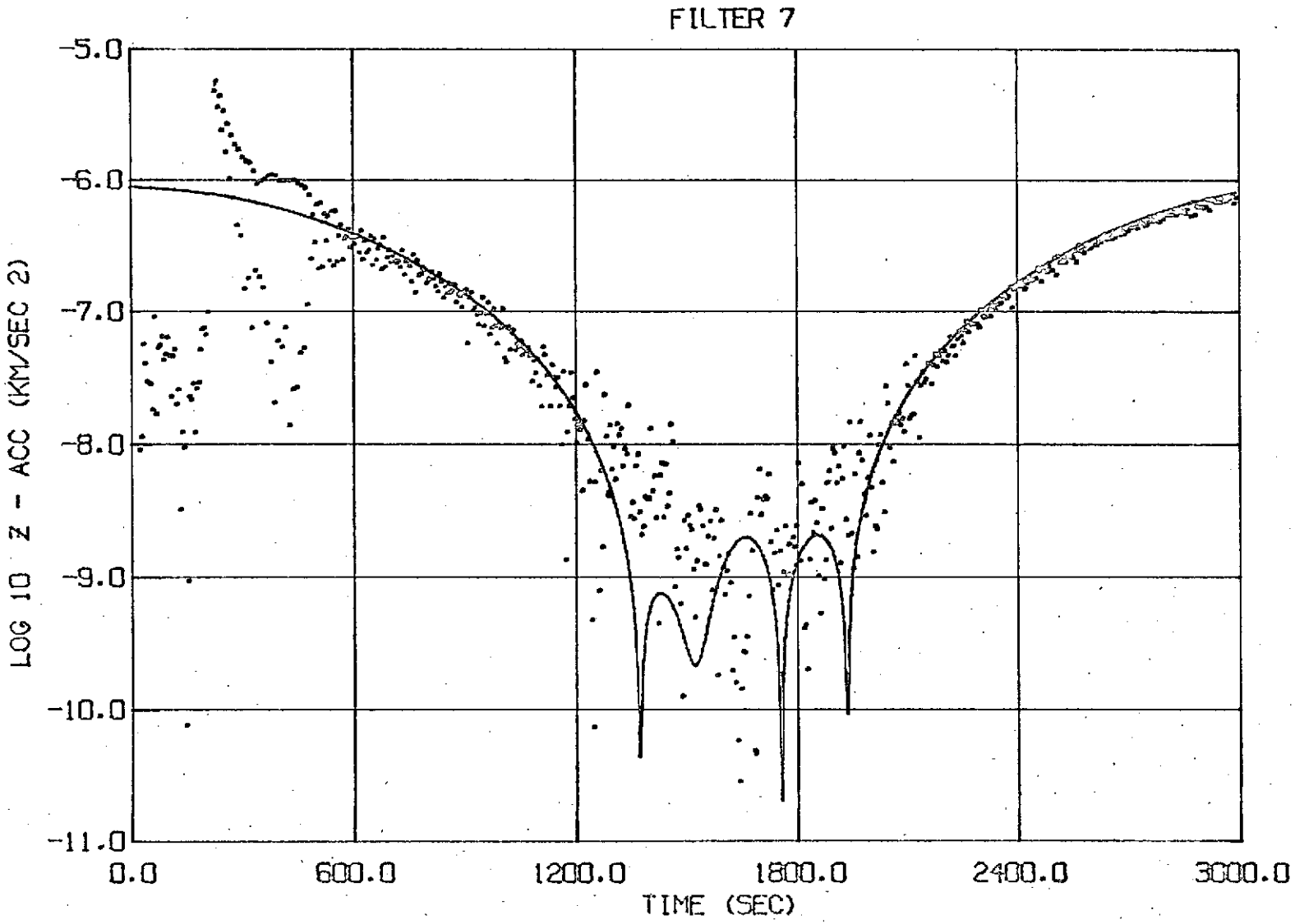

Figure 16. TRACKING THE z-ACCELERATION - LOG SCALE
($\hat{q}$; J_2, J_3 model; σ_ρ = 3cm, $\sigma_{\dot{\rho}}$ = 0.01 cm/sec)

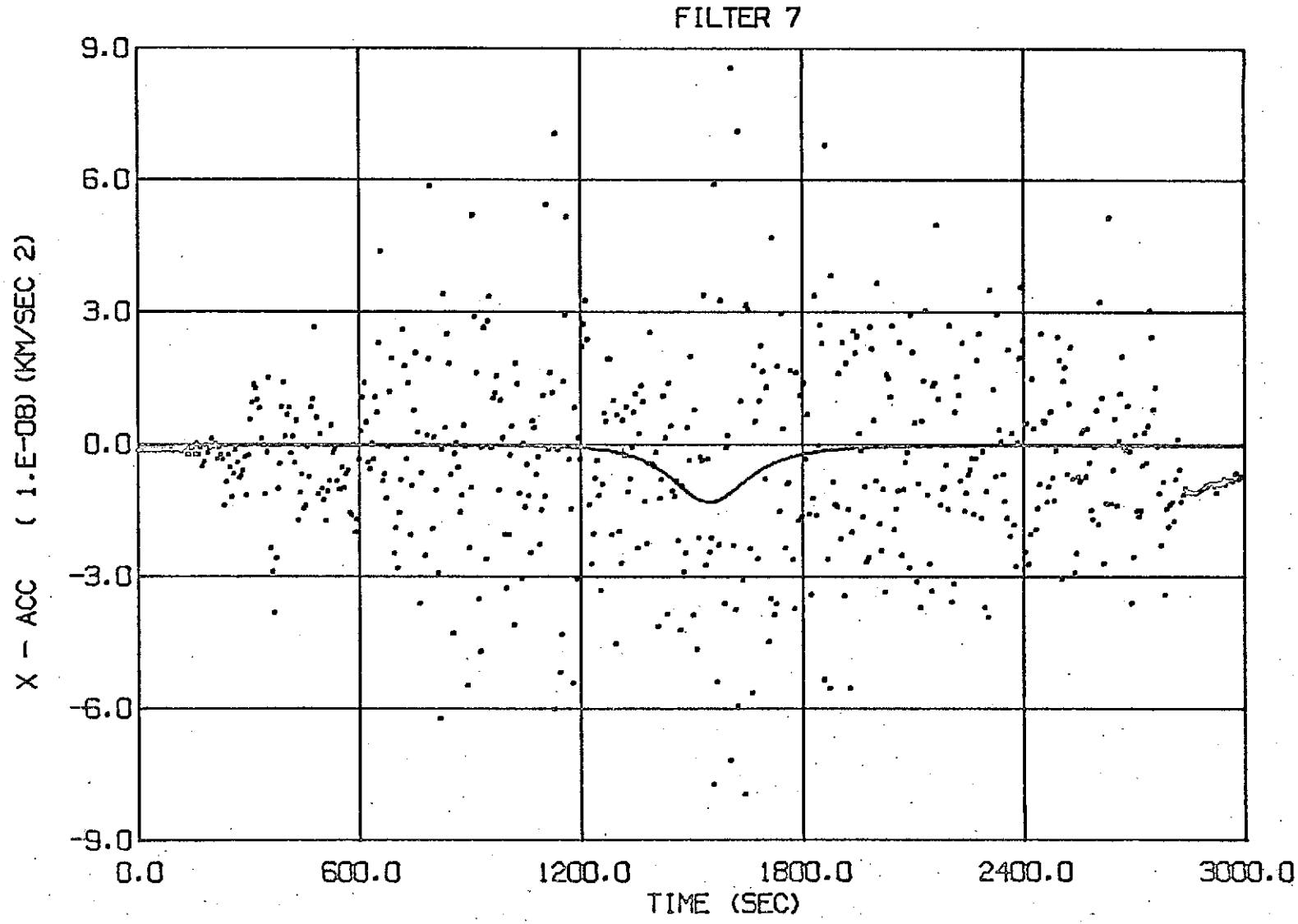

Figure 17. MASCON x-ACCELERATION

($\hat{q}$; Unmodeled mascon; σ_{ρ} = 1 cm, $\sigma_{\dot{\rho}}$ = 0.01 cm/sec)

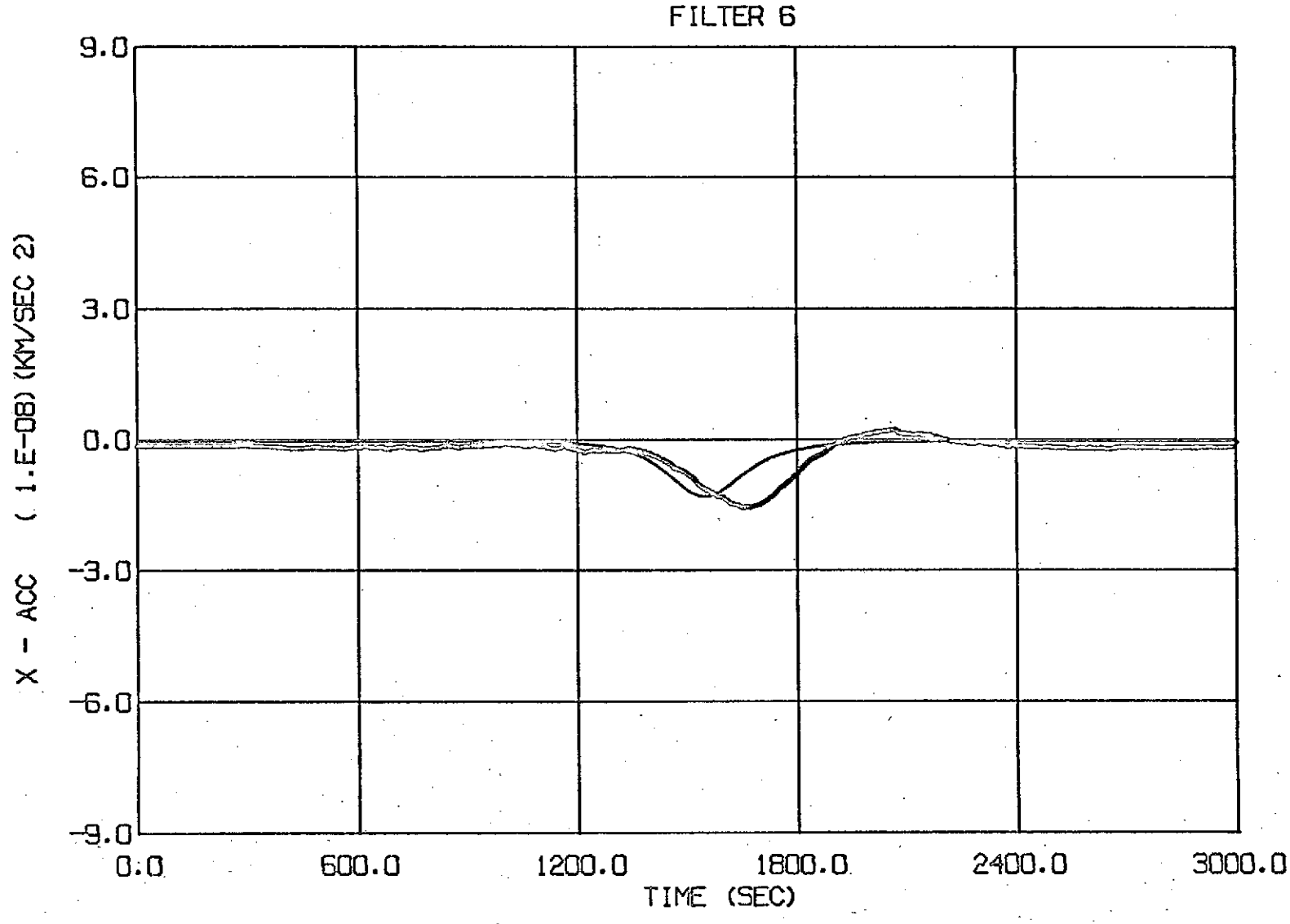

Figure 18. MASCON x-ACCELERATION

($\bar{U}$; Unmodeled mascon; σ_ρ = 1cm, $\sigma_{\dot{\rho}}$ = 0.01 cm/sec)

Table 1

SINGLE STATION PASS ERRORS

	Position Errors (m)			Velocity Errors (m/sec)		
	$x-\hat{x}$	$y-\hat{y}$	$z-\hat{z}$	$\dot{x}-\dot{\hat{x}}$	$\dot{y}-\dot{\hat{y}}$	$\dot{z}-\dot{\hat{z}}$
Perfect Model Extended Kalman	146.	-171.	- 9.8	0.22	-0.24	0.003
Uncompensated Extended Kalman	558.	-646.	-68.6	0.80	-0.95	-0.070
J - A - $\hat{q}$	150.	-118.	-335.	-0.69	-0.07	-1.34

VI. NEW TECHNOLOGY

The work under this contract consisted of the development of recursive estimation techniques for application to satellite orbit determination. The previously developed J-Adaptive estimator was modified and extended to include the geometry of random (unmodeled) accelerations, and the adaptive estimation of noise statistics in a stochastic model for these accelerations. The algorithms developed were tested by computer simulation on satellite orbit problems with unmodeled earth oblateness and mascon accelerations of various types.

The algorithm developed as a result of this effort is applicable to satellite orbit determination when excellent, continuous tracking coverage is available, as may be the case in satellite-to-satellite tracking.

Frequent reviews and a final survey for new technology were performed. While the extensions to the J-Adaptive estimator developed represent new mathematical techniques applicable to satellite orbit determination, it is believed that they do not represent reportable or patentable items within the meaning of the New Technology Clause. Our reviews and final survey found no other items which could be considered reportable items under the New Technology Clause.

VII. CONCLUSIONS AND RECOMMENDATIONS

Simulations demonstrate that the J-Adaptive estimator with estimated noise statistics can automatically, without human intervention, and with a very simple orbit model (e.g. two-body model), estimate satellite orbits to an accuracy comparable with the data noise levels, when excellent, continuous tracking coverage is available. Such tracking coverage may be available from satellite-to-satellite tracking. The fact that a two-body model can be utilized in the estimator prediction equation eliminates the need for numerical integration of the orbit dynamics equations, which in turn results in a very fast (computational) orbit estimation algorithm.

This estimator also tracks (estimates) the unmodeled acceleration vector. From these latter estimates a parametric model of the unmodeled accelerations may be recovered. The precision of tracking of these unmodeled accelerations is a function of the measurement noise levels (measurement precision). Everything else being equal, the J-Adaptive estimator with a priori "engineered" unmodeled acceleration statistics can track the unmodeled accelerations with higher precision than the estimator with estimated noise statistics. However, to engineer these statistics requires trial runs and simulations.

In the absence of excellent tracking station coverage (single station pass), the J-Adaptive estimator is unsuccessful; there is a relatively long transient before the estimator locks onto the unmodeled acceleration. A consider version of the estimator ("adaptive consider mode") shows some promise in this situation, but further research is required in this area.

On the basis of study results, the following recommendations are made:

(1) The J-Adaptive estimator with estimated noise statistics should be applied to the satellite-to-satellite tracking problem. Simulations should be performed in this environment to verify estimator performance. This is a very natural application because of the great abundance of data available. This abundance of data is precisely where the J-Adaptive estimator is extremely efficient as opposed to batch estimation methods.

(2) The J-Adaptive estimator should be studied in an environment containing more realistic measurement error models, including station location errors, timing errors, and so on.

(3) The single station pass tracking situation should be investigated, with a view, for example, to restricting uncertainties to selected subspaces of the state space.

(4) Other measurement types (angles) should be incorporated in J-Adaptive estimator studies. These may enhance the noise statistics estimation, thus improving tracking performance.

(5) Finally, parametric model recovery from the unmodeled acceleration estimates generated by the J-Adaptive estimator should be studied.

VIII. REFERENCES

1. Andrew H. Jazwinski and Conrad Hipkins, "Adaptive Estimation for Model Enhancement in Satellite Orbit Determination," Business and Technological Systems, Inc., BTS-TR-72-1, (Final Report under NAS 5-22011), July 1972.

2. A. H. Jazwinski, "Adaptive Sequential Estimation with Applications," Presented at the Fifth IFAC Symposium on Automatic Control in Space, Genoa, Italy, June 1973 (To appear in March 1974 issue of IFAC Journal-Automatica).

3. A. H. Jazwinski, "Adaptive Filtering," IFAC Journal-Automatica, Vol 5, pp. 475-485, July 1969.

4. A. H. Jazwinski, Stochastic Processes and Filtering Theory (book), Academic Press, Inc., New York, 1970.

Appendix A - Oblateness Model

A low order earth oblateness model utilized in the simulation studies is given below. In the equations which follow, $R = [x,y,z]^T$ is the satellite earth-fixed position vector expressed in km; $r = |R|$; μ is the gravitational parameter of the earth; J_2, J_3 and J_4 are zonal harmonic coefficients; C_{22}, S_{22}, C_{31}, S_{31}, C_{33}, S_{33} are tesseral harmonic coefficients; and

$$e_x = \begin{bmatrix} 1 \\ 0 \\ 0 \end{bmatrix} , \quad e_y = \begin{bmatrix} 0 \\ 1 \\ 0 \end{bmatrix} , \quad e_z = \begin{bmatrix} 0 \\ 0 \\ 1 \end{bmatrix} .$$

Defining the acceleration terms

$$F_{J2} = \frac{3\mu J_2}{2r^5} \left\{ \left[5 \left(\frac{z}{r}\right)^2 - 1 \right] R - 2ze_z \right\}$$

$$F_{J3} = \frac{\mu J_3}{2r^5} \left\{ \left[35 \left(\frac{z}{r}\right)^2 - 15 \right] \frac{zR}{r^2} - \left[15 \left(\frac{z}{r}\right)^2 - 3 \right] e_z \right\}$$

$$F_{J4} = \frac{15\mu J_4}{8r^7} \left\{ \left[21 \left(\frac{z}{r}\right)^4 - 14 \left(\frac{z}{r}\right)^2 + 1 \right] R + \left[4 - \frac{28}{3} \left(\frac{z}{r}\right)^2 \right] ze_z \right\}$$

$$F_{22} = \frac{3\mu}{r^5} \left\{ \left[- \frac{5(x^2 - y^2)}{r^2} R + 2xe_x - 2ye_y \right] C_{22} + \left[- \frac{10xy}{r^2} R + 2xe_y + 2ye_x \right] S_{22} \right\}$$

$$F_{31} = \frac{3\mu}{2r^7} \left\{ \left[- \frac{7x}{r^2} (4z^2 - x^2 - y^2) R + (4z^2 - y^2 - 3x^2) e_x - 2xye_y + 8xye_z \right] C_{31} \right.$$

$$\left. + \left[- \frac{7y}{r^2} (4z^2 - x^2 - y^2) R - 2xye_x + (4z^2 - x^2 - 3y^2) e_y + 8yze_z \right] S_{31} \right\}$$

$$F_{33} = \frac{15\mu}{r^7} \left\{ \left[- \frac{7x}{r^2} (x^2 - 3y^2) R + 3 (x^2 - y^2) e_x - 6xye_y \right] C_{33} \right.$$

$$\left. + \left[- \frac{7y}{r^2} (3x^2 - y^2) R + 6xye_x + 3 (x^2 - y^2) e_y \right] S_{33} \right\}$$

the acceleration due to oblateness, in earth-fixed coordinates and expressed in km/sec^2 is given by

$$\ddot{\Delta R}_{OE} = F_{J2} + F_{J3} + F_{J4} - F_{22} - F_{31} - F_{33}$$

Numerical values for the coefficients above are

$$\mu = 3.986032 \times 10^{5} \quad (km^3/sec^2)$$

$$J_2 = 1.08265 \times 10^{-3} \; R_E^2 \quad (km^2)$$

$$J_3 = -2.546 \times 10^{-6} \; R_E^3 \quad (km^3)$$

$$J_4 = -1.649 \times 10^{-6} \; R_E^4 \quad (km^4)$$

$$C_{22} = 0.1536 \times 10^{-5} \; R_E^2 \quad (km^2)$$

$$S_{22} = -0.872 \times 10^{-6} \; R_E^2 \quad (km^2)$$

$$C_{31} = 0.2091 \times 10^{-5} \; R_E^3 \quad (km^3)$$

$$S_{31} = 0.287 \times 10^{-6} \; R_E^3 \quad (km^3)$$

$$C_{33} = 0.782 \times 10^{-7} \; R_E^3 \quad (km^3)$$

$$S_{33} = 0.226 \times 10^{-6} \; R_E^3 \quad (km^3)$$

$$R_E = 6378.1641 \quad (km)$$